



Universiteit
Leiden
The Netherlands

The effects of breast cancer therapy on estrogen receptor signaling throughout the body

Droog, M.

Citation

Droog, M. (2017, June 8). *The effects of breast cancer therapy on estrogen receptor signaling throughout the body*. Retrieved from <https://hdl.handle.net/1887/49509>

Version: Not Applicable (or Unknown)

License: [Licence agreement concerning inclusion of doctoral thesis in the Institutional Repository of the University of Leiden](#)

Downloaded from: <https://hdl.handle.net/1887/49509>

Note: To cite this publication please use the final published version (if applicable).

Cover Page



Universiteit Leiden



The handle <http://hdl.handle.net/1887/49509> holds various files of this Leiden University dissertation

Author: Droog, Marjolein

Title: The effects of breast cancer therapy on estrogen receptor signaling throughout the body

Issue Date: 2017-06-08

Chapter 3

Comparative Cistromics Reveals Genomic Cross-talk between FOXA1 and ER α in Tamoxifen-Associated Endometrial Carcinomas

Marjolein Droog, Ekaterina Nevedomskaya*, Yongsoo Kim*, Tessa Severson, Koen D. Flach, Mark Opdam, Karianne Schuurman, Patrycja Gradowska, Michael Hauptmann, Gwen Dackus, Harry Hollema, Marian Mourits, Petra Nederlof, Hester van Boven, Sabine C. Linn, Lodewyk F.A. Wessels, Flora E. van Leeuwen and Wilbert Zwart

*equal contributions

Cancer Res. 76 (2016) 3773-3784

Abstract

Tamoxifen, a small-molecule antagonist of the transcription factor estrogen receptor alpha (ER α) used to treat breast cancer, increases risks of endometrial cancer. However, no parallels of ER α transcriptional action in breast and endometrial tumors have been found that might explain this effect. In this study, we addressed this issue with a genome-wide assessment of ER α -chromatin interactions in surgical specimens obtained from patients with tamoxifen-associated endometrial cancer.

ER α was found at active enhancers in endometrial cancer cells as marked by the presence of RNA polymerase II and the histone marker H3K27Ac. These ER α binding sites were highly conserved between breast and endometrial cancer and enriched in binding motifs for the transcription factor FOXA1, which displayed substantial overlap with ER α binding sites proximal to genes involved in classical ER α target genes.

Multifactorial ChIP-seq data integration from the endometrial cancer cell line Ishikawa illustrated a functional genomic network involving ER α and FOXA1 together with the enhancer-enriched transcriptional regulators p300, FOXM1, TEAD4, FNFIC, CEBP8, and TCF12. Immunohistochemical analysis of 230 primary endometrial tumor specimens showed that lack of FOXA1 and ER α expression was associated with a longer interval between breast cancer and the emergence of endometrial cancer, exclusively in tamoxifen-treated patients.

Our results define conserved sites for a genomic interplay between FOXA1 and ER α in breast cancer and tamoxifen-associated endometrial cancer. In addition, FOXA1 and ER α are associated with the interval time between breast cancer and endometrial cancer only in tamoxifen-treated breast cancer patients.

Abbreviations

ChIP-seq, Chromatin Immunoprecipitation coupled with massive parallel sequencing; CEAS, cis-regulatory element annotation system; CPM, in counts per million; DEX, dexamethasone; E2, estradiol; ER α , estrogen receptor alpha; EtOH, ethanol; FOXA1, Forkhead box protein A1; FPKM, fragments per kilobase of exon per million fragments mapped; IPA, Ingenuity Pathway Analysis; NR3C1, Glucocorticoid Receptor; RNA Pol II, RNA polymerase II; TAMARISK, Tamoxifen Associated Malignancies: Aspects of RISK; TMA, tissue microarray.

Introduction

Of all breast tumors, roughly 75% depend on ER α for cell proliferation and tumor progression. Consequently, most breast cancer treatment modalities are aimed to inhibit ER α activity. Tamoxifen is the most widely applied hormonal therapy, which acts through competitive inhibition of ER α 's natural ligand estrogen¹. Although tamoxifen inhibits ER α in breast cells, it stimulates ER α in certain other tissues, including the endometrium, specifically in a low estrogen environment, i.e., postmenopausal women^{2–6}.

Due to tissue-selective action of tamoxifen, postmenopausal breast cancer patients on this drug have an increased risk of endometrial cancer development by 2- to 7-fold, depending on the duration of use^{4,5,7,8}. This increased ER α activity was linked with an altered expression level of coactivator SRC1⁹ and PAX2¹⁰ in endometrial cancer cells. However, manipulating expression levels of either SRC1 or PAX2 in breast cancer cell line models did not support these findings^{11,12}, implying that these proteins are not the sole drivers of agonistic features of tamoxifen observed in endometrial tissue. In addition, ER α transcriptional regulation in endometrial cancer has exclusively been studied using cell lines¹³ while ER α genomic behavior in primary human endometrial tumors remains unexplored.

For ER α to bind the chromatin in breast cancer cells, it requires FOXA1^{14–16}. FOXA1 is a pioneer factor, regulating chromatin accessibility and thereby enables ER α -dependent gene activation and proliferation of breast cancer cells¹⁴. FOXA1 was previously identified as one of the luminal breast cancer–defining transcription factors^{17,18}, and its expression correlates with a favorable outcome in breast cancer^{19–21}. In ER α -negative breast cancer cells, exogenous introduction of ER α and FOXA1 along with GATA3 was sufficient to reprogram these cells toward hormone responsiveness²². Cumulatively, these reports position FOXA1 as a crucial player in ER α functionality in breast cancer. In endometrial cancer, the pioneer factor for ER α is unknown, and the mechanisms that dictate ER α action in this tissue remain elusive.

To study the genomic features of ER α in endometrial tumors, we performed chromatin immunoprecipitation sequencing (ChIP-seq) in surgical samples from five endometrial tumors of patients who were previously treated with tamoxifen. ER α binding sites in endometrial tumors were enriched for RNA polymerase II as well as for H3K27Ac, the posttranslational histone modification that marks both active promoters and active enhancers. Overlap of ER α chromatin binding sites was observed between breast tumors and endometrial cancers. In addition, we identified a genomic functional network in the endometrial cancer cell line Ishikawa, implicating FOXA1 and ER α as part of a large multiprotein transcriptional network that enrolls FOXM1, TEAD4, and TCF12. The direct clinical implications of this coordinated action between ER α and FOXA1

in endometrial carcinogenesis was assessed for 230 endometrial cancer patients who were previously treated for breast cancer. In contrast to ER α , FOXA1 expression did not correlate with endometrial cancer patient survival. Interestingly, both ER α and FOXA1 expression did associate with short interval between breast cancer treatment and endometrial cancer diagnosis, exclusively for the patients who received tamoxifen.

With this, we present a genomic conservation of ER α action between breast and endometrial tumor specimens that highlights FOXA1 as a common player of hormonal response in both tissues.

Materials and Methods

Patient Series

Endometrial tumor tissue from 230 patients of the Tamoxifen Associated Malignancies: Aspects of RISK (TAMARISK) study was analyzed as described before^{5,7,23}. Clinicopathologic parameters from endometrial cancers can be found in Supplementary Table S1. Tumor samples were analyzed anonymously, with coded leftover material that cannot be traced back to the patients that these materials originated from. This study was performed in accordance with the Code of Conduct of the Federation of Medical Scientific Societies in the Netherlands (<http://www.fmwv.nl>). The study has been approved by the local medical ethics committee of the Netherlands Cancer Institute.

ChIPs and Analyses

ChIPs were performed as described previously^{24,25} on endometrioid and endocarcinoma tumors that are part of the TAMARISK study^{5,7,23}. These endometrial tumors were collected from patients who were still on tamoxifen on the day of surgery or had stopped 1 to 2 months prior to surgery. Clinicopathologic parameters can be found in Supplementary Table S2. Tumor samples were cryosectioned, fixed in 1% formaldehyde for 20 minutes, and processed for sonication. For each ChIP, 10 μ g of antibody, and 100 μ L of Protein A (for ER α and H3K27ac) and Protein G (for FOXA1 and RNA polymerase II) magnetic beads (Invitrogen) were used. Antibodies raised to detect ER α (SC-543; Santa Cruz Biotechnology), RNA polymerase II (ab5408; Abcam), H3K27ac (39133; Active Motif), and FOXA1/2 (SC-6554; Santa Cruz Biotechnology) were used. The specificity of SC-6554 antibody to detect FOXA1 was verified using immunoprecipitation followed by Western blot using specific antibodies (Seven Hills, WMAB-2F83 and WRAB-1200; Supplementary Figure S1). Primer sequences used for ChIP-qPCR are listed in Supplementary Table S3. All Ishikawa ChIP-seq and RNA-seq datasets were generated by the ENCODE consortium, and

Supplementary Table S4 shows all accession numbers of the used datasets that also includes breast cancer ER α ChIP-seq data from Jansen and colleagues²⁵. Patient characteristics of breast cancer tumors can be found in Supplementary Table S5.

Illumina Sequencing and Enrichment Analysis

ChIP DNA was amplified as described²⁶. Sequences were generated by the Illumina Hiseq 2000 genome analyzer (using 50-bp reads) and aligned to the Human Reference Genome (assembly hg19, February 2009). Reads were filtered based on MAPQ quality (reads with MAPQ>20) to eliminate reads from repetitive elements. Peak calling was performed over input, using Dfilter²⁷ and MACS peak caller version 1.4²⁸. Only peaks identified using both algorithms were considered. MACS was run with the default parameters, except $P = 10^{-7}$. DFilter was run using settings bs = 50, ks = 30, refine, nonzero. Details on the number of reads obtained and the percentage of reads aligned, and number of peaks called can be found in Supplementary Table S6. Details on bioinformatics analyses can be found in the Supplementary Methods.

RNA Isolation and mRNA Expression

RNA from tumors was isolated using the AllPrep DNA/RNA/miRNA Universal Kit (Qiagen). cDNA was synthesized with Superscript III Reverse Transcriptase (Invitrogen), using random hexamer primers. RT-PCR was performed using SYBR Green (GC Biotech) on a Roche Lightcycler, using 50 cycles of amplification for all genes tested. RT-PCR products were detected by agarose gel electrophoresis. Primer sequences are listed in Supplementary Table S7.

Immunohistochemistry and Tissue Microarray Analyses

For immunohistochemical analysis, an antibody for FOXA1 was applied (2F83, Seven Hills Bioreagents). This antibody was previously reported to be highly specific for FOXA1²⁹. Antibody specificity was confirmed by Western blot (Supplementary Figure S1). Immunohistochemistry on the TAMARISK tissue microarray (TMA) was performed using a Ventana Benchmark Ultra system, applying standard protocols. A kappa of 0.78 was calculated from scoring of two independent observers. ER α staining was previously performed as described⁷. Patients were categorized based on ER α and FOXA1 expression levels (at 10% cutoff) and stratified over tamoxifen use. The mean time interval between breast and endometrial cancer diagnosis was compared between the groups and significance

of the differences was assessed using the t-test. For survival analysis, Kaplan–Meier survival plots were generated categorizing for ER α and FOXA1 expression levels and stratifying over tamoxifen use.

Data Access

All sequencing data can be found at GEO (GSE81213).

Results

ER α is Found at Active Enhancers in Human Endometrial Tumor Specimens

Tamoxifen exposure increases endometrial cancer risk⁵. The genomic features of ER α in relation to tamoxifen in endometrial tumor specimens remain unexplored. To investigate tamoxifen-associated endometrial cancer⁵, five endometrial tumors were analyzed from postmenopausal patients who received tamoxifen to treat breast cancer (Figure 1; Supplementary Table S2 for patient details). Endometrioid adenocarcinomas were selected because these are generally ER α -positive, irrespective of whether the endometrial tumor was spontaneous or tamoxifen associated⁷.

For all five tumors, ChIP-seq was performed for ER α as well as RNA polymerase II and H3K27Ac, which marks histones both at active promoters and active enhancers (Figure 1A). Only for tumor D, H3K27Ac ChIP-seq data were absent. Consistently between all tumors, ER α sites were co-occupied by H3K27Ac and RNA polymerase II (exemplified in Figure 1B, shown genome-wide in Figure 1C and quantified in Figure 1D). For tumors C and E, RNA polymerase II signal was relatively low at ER α sites (Figure 1B), but still quantifiably detected and enriched over background (Figure 1C and D). ChIP-seq peaks were successfully validated by ChIP-qPCR for all three factors (Supplementary Figures S2A–S2C). Experiments were technically reproducible, with considerable overlap between replicates for the same tumor (ER α : Pearson correlation coefficient = 0.68; H3K27Ac: Pearson correlation coefficient = 0.88; see Supplementary Figures S3A–S3C). Between two sections from the same tumor, RNA polymerase II ChIP-seq was more variable (Pearson correlation coefficient = 0.41), suggesting intratumor heterogeneity of this factor. Analogous to what was previously reported in breast cancer specimens^{25,30}, endometrial ER α is rarely found at promoters and mainly binds distal intergenic regions and introns (Figure 1E). Cumulatively, these data illustrate that ER α in tamoxifen-associated endometrial tumor specimens shows the same pattern as previously identified in breast cancer, mainly occupying active enhancer regions, positive for both H3K27Ac and RNA polymerase II (Figure 1F).

Conservation of ER α /Chromatin Binding between Surgical Specimens of Breast and Endometrial Cancer Patients

ER α binds active enhancer regions in endometrial tumors, analogous to what was found in breast cancer. To assess any potential overlap in the chromatin binding distributions of ER α between both tumor types, ChIP-seq data from the five endometrial cancers (Figure 1) were compared with publicly available ER α ChIP-seq datasets we previously generated from five breast tumors (Figure 2A; ref.25). As exemplified, robust ER α ChIP-seq signal was detected for both tumor types in all 10 tumors (Figure 2B). Consistent with previous reports in breast cancer^{25,30}, a number of ER α binding sites greatly deviated between tumor samples, as we now also show in endometrial tumors (Figure 2C). In total, 9,507 ER α interaction sites were found in at least 2 out of 5 breast cancers, while 12,771 ER α sites were found shared in at least 2 out of 5 endometrial cancers. Between the two tumor types, 3,074 ER α sites were shared (Figure 2C).

ER α sites shared between breast cancer and endometrial cancer were robust as illustrated in a heatmap (Figure 2D, for quantification see Supplementary Figure S4). To identify any potential transcriptional regulators that interact with ER α at these sites, conserved chromatin binding events between endometrial and breast tumors were mined for enriched motifs (Figure 2E). As expected, ER α binding sites in both endometrial and breast tumors were strongly enriched for ESR1 motifs ($-\log_{10}P = 690.776$). Interestingly, FOXA1 motifs were also found highly enriched at ER α binding sites in both tumor types ($-\log_{10}P = 342.067$). FOXA1 is classically known to facilitate ER α /chromatin interactions in breast cancer^{15,16}, but our findings suggest that FOXA1 may play a role for ER α functioning in tamoxifen-associated endometrial cancer as well.

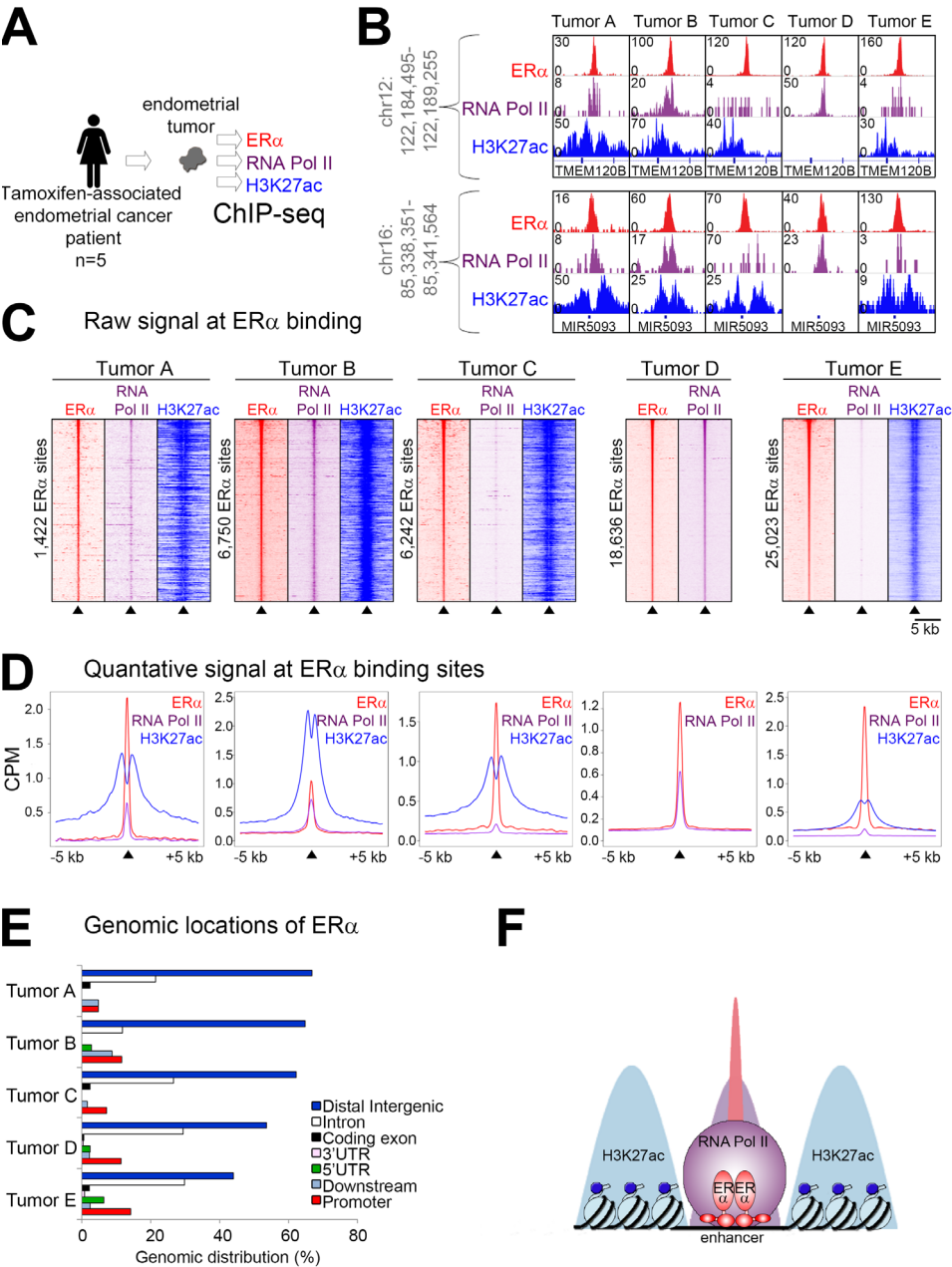


Figure 1. ER α binds to active enhancers in tamoxifen-associated endometrial tumor specimens.

- A)** Experimental overview. Tumor samples from five endometrial cancer patients were used to ChIP-seq ER α , RNA polymerase II (RNA Pol II), and H3K27ac.
- B)** Snapshots depicting ChIP-seq data for ER α (red), RNA polymerase II (purple) and H3K27Ac (blue) from five different endometrial tumor specimens. Genomic locations and read counts are shown.

Genomic Interactions of FOXA1 and ER α in Endometrial Tumor Specimens

FOXA1 motifs were enriched at ER α binding sites present in both breast and endometrial cancer samples. Immunohistochemistry analysis validated ER α and FOXA1 expression in both tumor types (Figure 3A). This was previously reported by others for breast cancer^{30, 31} as well as endometrial cancer^{32–34}. Next, we performed ChIP-seq for FOXA1 in the five endometrioid adenocarcinoma specimens that were previously used to ChIP ER α , RNA polymerase II, and H3K27ac. We directly compared these FOXA1 binding patterns with ER α profiles within the same tumor (Figure 3B).

For tumor D, FOXA1 ChIP-seq signal was not observed (tested in two biologic replicates), nor did we detect its mRNA expression (Supplementary Figure S5). FOXA1 binding sites as identified by ChIP-seq could successfully be validated by ChIP-qPCR (Supplementary Figure S2D). Furthermore, FOXA1 ChIP-seq was technically robust (Pearson correlation coefficient = 0.67; Supplementary Figure S3D). ER α and FOXA1 were found at overlapping genomic locations in all tested tamoxifen-associated endometrioid adenocarcinomas, which were also shared with the endometrioid adenocarcinoma cancer cell line Ishikawa (Figure 3B and C, quantified in D).

For FOXA1, 549 sites were shared between two out of four endometrial tumors. For ER α , 4,623 sites were shared in at least three out of five tumors (Figure 3C and D). However, raw data analyses illustrated that at ER α binding sites, FOXA1 signal was generally observed at the same genomic regions. This suggests that false negativity was observed due to the peak-calling threshold. Analogous to these findings, FOXA1 sites were commonly positive for ER α (Figure 3C and quantified in Figure 3D). Next, potential interacting transcriptional regulators were identified by motif enrichment analysis. As expected, forkhead motifs and ESR motifs were found for regions bound by ER α as well as FOXA1 (Figure 3E). Furthermore, additional motifs were identified for transcription factors previously described to be involved in endometrial cancer, including androgen receptor³⁵, progesterone receptor³⁶, RORB³⁷, as well as SOX proteins³⁸. Cumulatively, these data implicate that FOXA1 binds to ER α sites in tamoxifen-associated endometrial cancer that are potentially co-occupied by other transcription factors.

- C)** Heatmap depicting raw reads of ChIP-seq data for ER α (red), RNA polymerase II (purple), and H3K27Ac (blue). ER α peaks are selected and sorted on intensity. Heatmaps are centered on the peak, showing reads within a 5 kb window around the peak.
- D)** Normalized average signal (in counts per million, CPM) of data shown in C.
- E)** Genomic distribution of ER α ChIP-seq peaks in five endometrial cancers.
- F)** Model for the genomic landscape of ER α in tamoxifen-associated endometrial tumors.

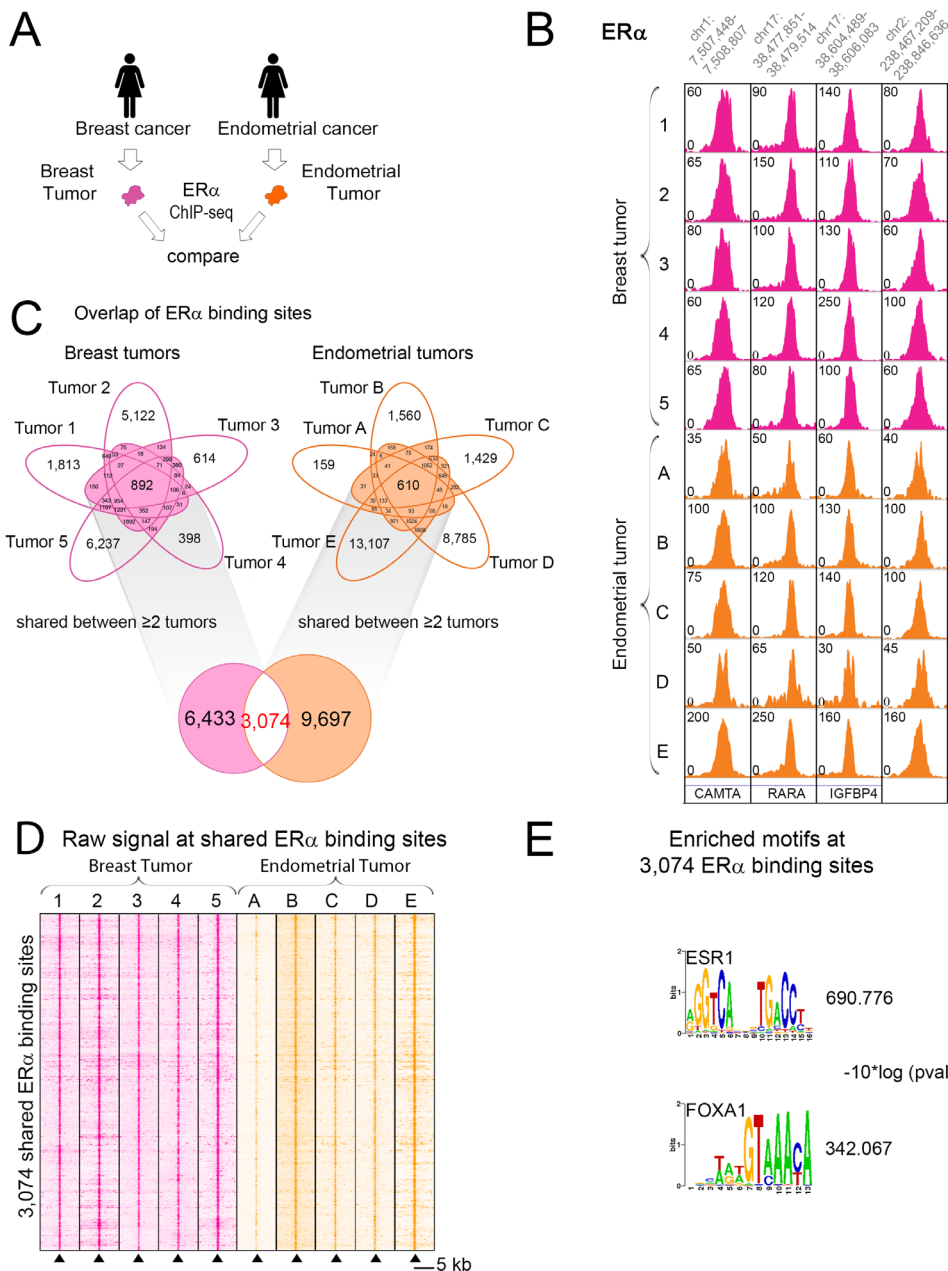


Figure 2. ERα chromatin binding landscape in tamoxifen-associated endometrial cancers and breast tumor samples.

A) Experimental overview. Tumor samples from five tamoxifen-associated endometrial cancer patients (orange) and five breast cancer patients (pink) were processed for ERα ChIP-seq and profiles were directly compared.

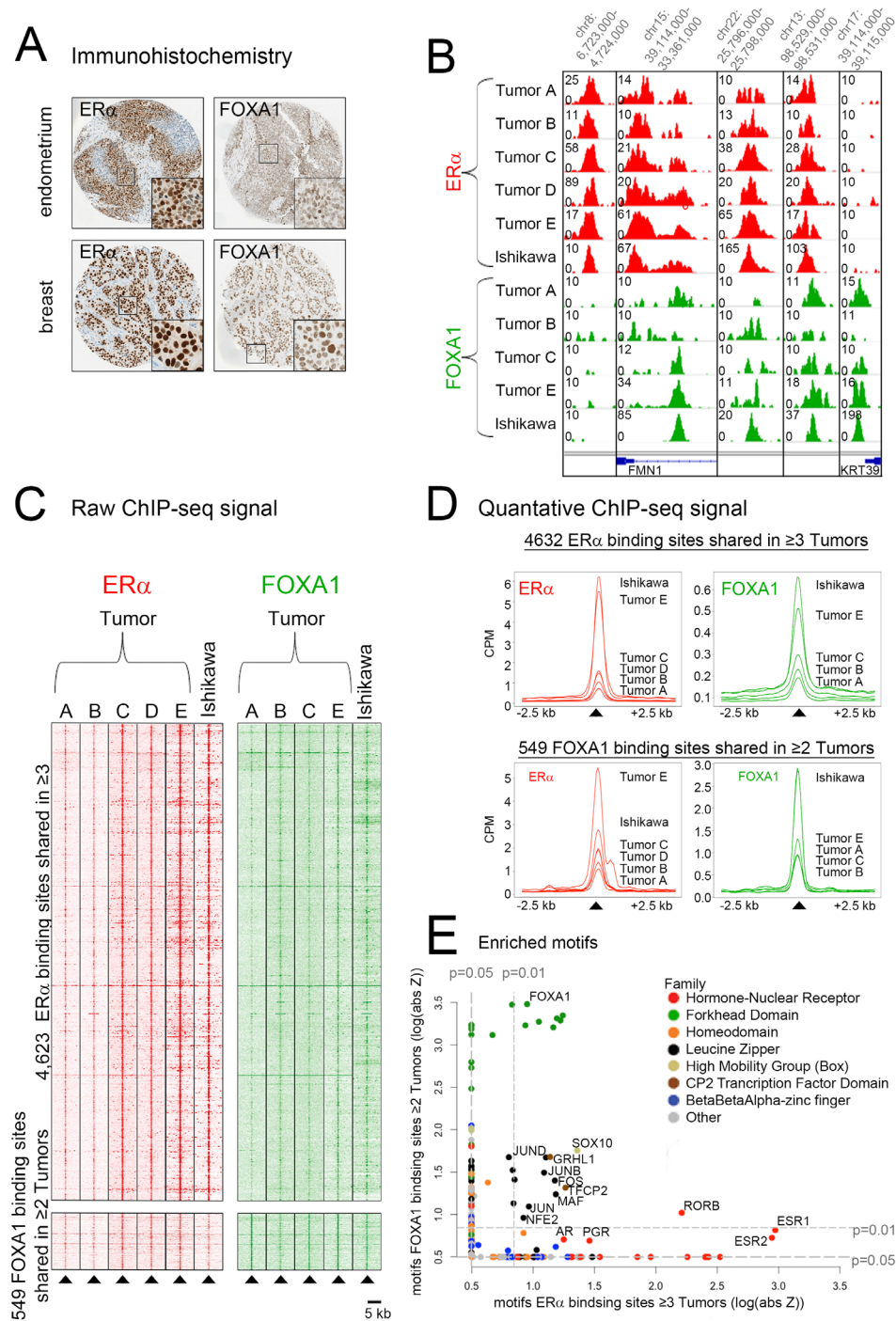
Endometrial FOXA1/ER α Sites Mark a Regulatory Transcription Factor Hub at Enhancers

Endometrial tumors express ER α as well as FOXA1, which share substantial overlap in binding sites. Importantly, ER α and FOXA1 chromatin binding profiles of Ishikawa cells are shared with primary endometrial tumor tissue samples, suggesting applicability of this cell line model to analyze the correlation between FOXA1 and ER α binding sites and to identify transcriptomic regulation at these sites (Figure 3). In Ishikawa, approximately 20% of FOXA1 binding sites overlap with ER α binding sites (Figure 4A), yielding a concise list of 599 shared ER α /FOXA1 binding sites in this cell line.

Compared to ER α unique binding sites and sites shared between ER α and FOXA1, the genomic regions uniquely bound by FOXA1 were markedly higher enriched at promoter regions (Figure 4B). Next, we analyzed DNA motifs in genomic regions bound exclusively by ER α , FOXA1, or shared by both transcription factors (Figure 4C). Sites shared by ER α and FOXA1 showed enrichment for ESR1 motifs as well as Forkhead transcription factors. As expected, ER α unique binding sites were devoid of Forkhead motifs, while FOXA1 unique sites lacked ESR1 motifs, suggesting no false negativity for the unique binding site subsets.

Apart from ER α and FOXA1 motifs, other transcription factors were found selectively enriched between the peak subsets. Substantial overlap was found between these motifs and those found in tumors (Figure 3E). Out of 106 motifs, 85 transcription factors were expressed in Ishikawa cells, based on publicly available RNA-seq data, which was generated as part of the ENCODE consortium (for accession numbers of used datasets see Supplementary Table S4). To provide experimental validation of the identified motifs, publicly available ChIP-seq datasets were used from Ishikawa cells (for GEO accession numbers see Supplementary Table S4). In accordance with the motif analyses, CTCF chromatin binding was found at FOXA1 sites, but not at ER α sites. Most other transcriptional regulators (TEAD4, EP300, FOXM1, MAX, NFIC, RAD21, SRF, TCF12, USF1) showed signal for unique regions of ER α and FOXA1, but was strongest at

- B)** Snapshots of ER α ChIP-seq signal in endometrial tumor tissue (orange) and breast tumor tissue (pink). Genomic locations and read count are shown.
- C)** Venn diagram visualizing shared and unique ER α chromatin binding events in five breast tumor samples (pink) and five endometrial tumor samples (orange). For each tumor type, the ER α peaks shared between at least two tumors were used. The number of overlapping peaks between the two tumor types is shown in red.
- D)** Heatmap visualization of the shared ER α binding sites between breast (pink) and endometrial (orange) tumor samples, as defined in C.
- E)** ER α binding sites shared between endometrial and breast tumor samples are enriched for ESR1 and FOXA1 motifs. Motifs sequence logos and P values are shown.



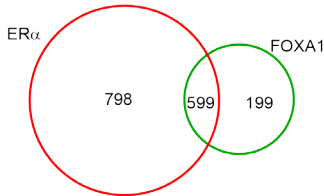
regions co-occupied by both FOXA1 and ER α (Figure 4D; Supplementary Figure S6 for quantifications). Furthermore, these transcription factors were tested for expression analysis in tamoxifen-associated cancers and Ishikawa cells (Supplementary Figure S5). All tested transcription factors were expressed in at least 3 out of 4 tumors and found expressed in Ishikawa cells. Genes that correspond to genomic regions bound by ER α and FOXA1 were identified (<20 kb upstream of transcriptional start site or within gene body; see Materials and Methods) and used for Ingenuity Pathway Analysis to reveal the network in which these proteins operate. As expected, ESR1 ($P = 8.71\text{E}-08$) was identified as a top upstream regulator. Accordingly, the top enriched network was centered around ESR1 (Figure 4E; Supplementary Table S8). All genes in this pathway were under control of ER α signaling, as identified by RNA-seq data integration from Ishikawa cells, treated for 4 hours with estradiol or vehicle control (Figure 4E; Supplementary Table S4).

To investigate the transcription factor context in which ER α and FOXA1 operate, we performed unsupervised hierarchical clustering based on the identified binding patterns for all analyzed transcriptional regulators, which resulted in the identification of distinct functional genomic clusters (Figure 4F). Cluster 1 was enriched for transcriptional regulators found at promoter regions (Figure 4G), such as RNA polymerase II, TAF1, YY1, MAX, EGR1, ZBTB7A, USF1, SRF, and CREB1 (Figure 4F). Cluster 2, which contained ER α and FOXA1 binding regions, was enhancer enriched (Figure 4G) and showed clustering among p300, FOXM1, NR3C1

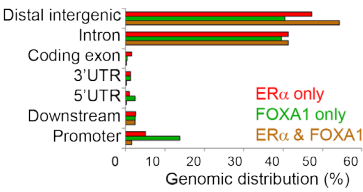
Figure 3. Chromatin binding patterns of ER α and FOXA1 in tamoxifen-associated endometrial tumor specimens.

- A)** Breast and endometrial tissues were stained by immunohistochemistry for ER α and FOXA1. Example of ER α and FOXA1 expression in breast and endometrial tumor tissues. Magnification, $\times 200$.
- B)** Snapshots of ChIP-seq data for ER α (red; five samples) and FOXA1 (green; four samples) in independent tamoxifen-associated endometrial tumors and the endometrial cancer cell line Ishikawa. Read count and genomic locations are shown.
- C)** Heatmap visualization of ER α (red) and FOXA1 (green) binding sites in tumors and the endometrial cancer cell line Ishikawa. For ER α , all 4,623 sites found in at least 3 out of 5 tumors were selected. For FOXA1, 549 sites were identified in at least 2 out of 4 tumors. All peaks identified for ER α (top) and FOXA1 (bottom) were analyzed separately, where raw data for ER α and FOXA1 ChIP-seq are shown. Raw read count of all peaks is vertically aligned on the center of the peak region.
- D)** Normalized average read count (CPM) of ChIP-seq data visualized in C. Data were centered on the peak regions and include a 2.5-kb window around the peak. The y-axis shows normalized read count.
- E)** Scatter plot showing motif enrichment analysis of ER α and FOXA1 ChIP-seq sites depicted in C and D. The individual dots represent the absolute Z-score of enriched motif in log-scale. Two vertical and horizontal dashed gray lines indicate the absolute Z-score corresponding to P value of 0.05 and 0.01 for ER α and FOXA1 binding sites, respectively.

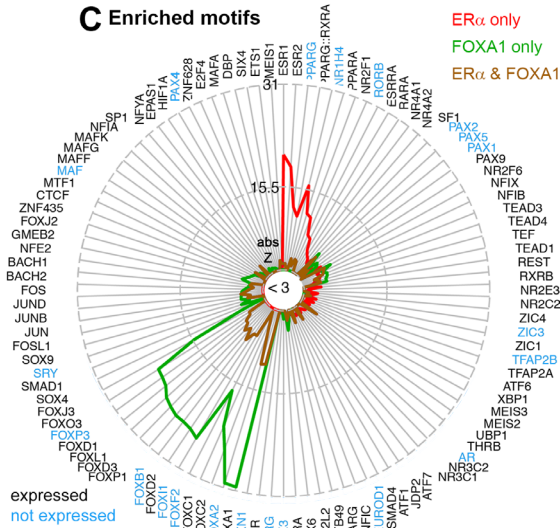
A Overlap of binding sites



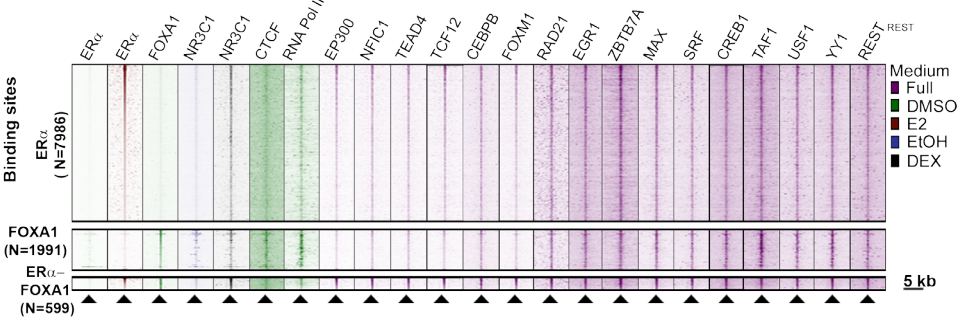
B Genomic distribution



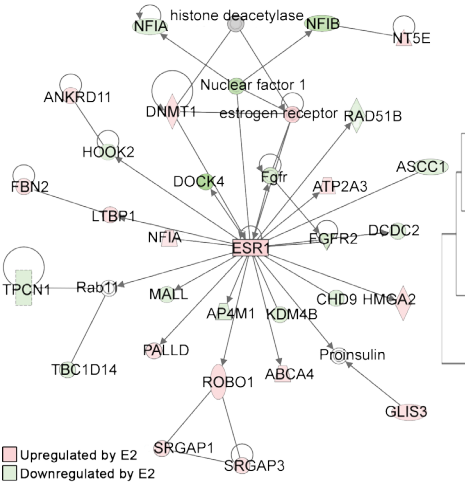
C Enriched motifs



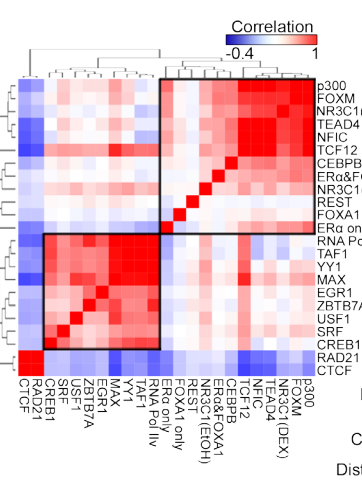
D Raw ChIP-seq signal



E Network model for binding sites of ERα & FOXA1



F Clustering of differential binding sites



G Genomic distribution



(Glucocorticoid Receptor), TEAD4, NFIC, TCF12, and CEBPB. These cell line data are in agreement with primary tumor data where ER α was found to bind active enhancers (Figure 1). Cumulatively, these data implicate genomic locations shared by ER α and FOXA1 as central genomic hubs for enhancer action, where multiple transcriptional regulators bind proximal to genes involved in classical estrogen-regulated processes.

Interplay of FOXA1 and ER α in Tamoxifen-associated Endometrial Cancer

ER α 's functional activity is linked with FOXA1 in tamoxifen-associated endometrial cancer. We next determined the potential clinical implications of the interplay of FOXA1 and ER α in this context (Figure 5), using TMAs from the TAMARISK study⁷. The TAMARISK study involves samples from 230 endometrial tumors that were collected from patients who were previously diagnosed with breast cancer, half of whom received tamoxifen (Figure 5A; Supplementary Table S1). We assessed the interval time between breast cancer diagnosis and endometrial cancer diagnosis as well as endometrial cancer-related survival. These clinical variables were

Figure 4. Comparative genomics between ER α and FOXA1 in endometrial cancer cells Ishikawa.

- A)** Venn diagram visualizing overlap between chromatin binding events for ER α (red) and FOXA1 (green).
- B)** Genomic distribution of sites bound by either ER α alone (red), FOXA1 alone (green), or shared by ER α and FOXA1 (brown).
- C)** Radar plot, visualizing DNA motif enrichment for genomic sites bound by either ER α (red) or FOXA1 (green) alone, or by both (brown). The radial data points represent the absolute value of Z-score. The lower bound of the abs Z-score is 3, which corresponds to a P value of 0.00135. Genes expressed in Ishikawa [genes with fragments per kilobase of exon per million fragments mapped (FPKM) > 1] are in black, while genes not expressed are in blue.
- D)** Heatmap visualization of ChIP-seq ENCODE data for several transcriptional regulators at sites bound by ER α and/or FOXA1. Raw read count of all peaks was vertically aligned, and data were centered on the center of the peak region. Colors correspond to different treatments; cells were either grown in full medium (purple) or hormone deprived, followed by a 1-hour incubation of either DMSO (green), 10 nM estradiol (E2, brown), ethanol (EtOH, blue), or 100 nM dexamethasone (DEX, black).
- E)** Ingenuity Pathway Analysis depicts the top-network model of genes with a shared ER α /FOXA1 site within the gene body or within 20k upstream of the transcriptional transcription start site. The node color indicates the FPKM fold change in Ishikawa cells upon a 4-hour estradiol (E2) stimulation, being either upregulated (red) or downregulated (green) related to control.
- F)** Unsupervised clustering of binding sites of all available transcriptional regulators. FOXA1 unique, ER α unique, and shared ER α /FOXA1 sites are analyzed separately. Red, positive correlation; blue, negative correlations.
- G)** Genomic distribution of peaks shared between at least four out of nine proteins in either cluster 1 or cluster 2.

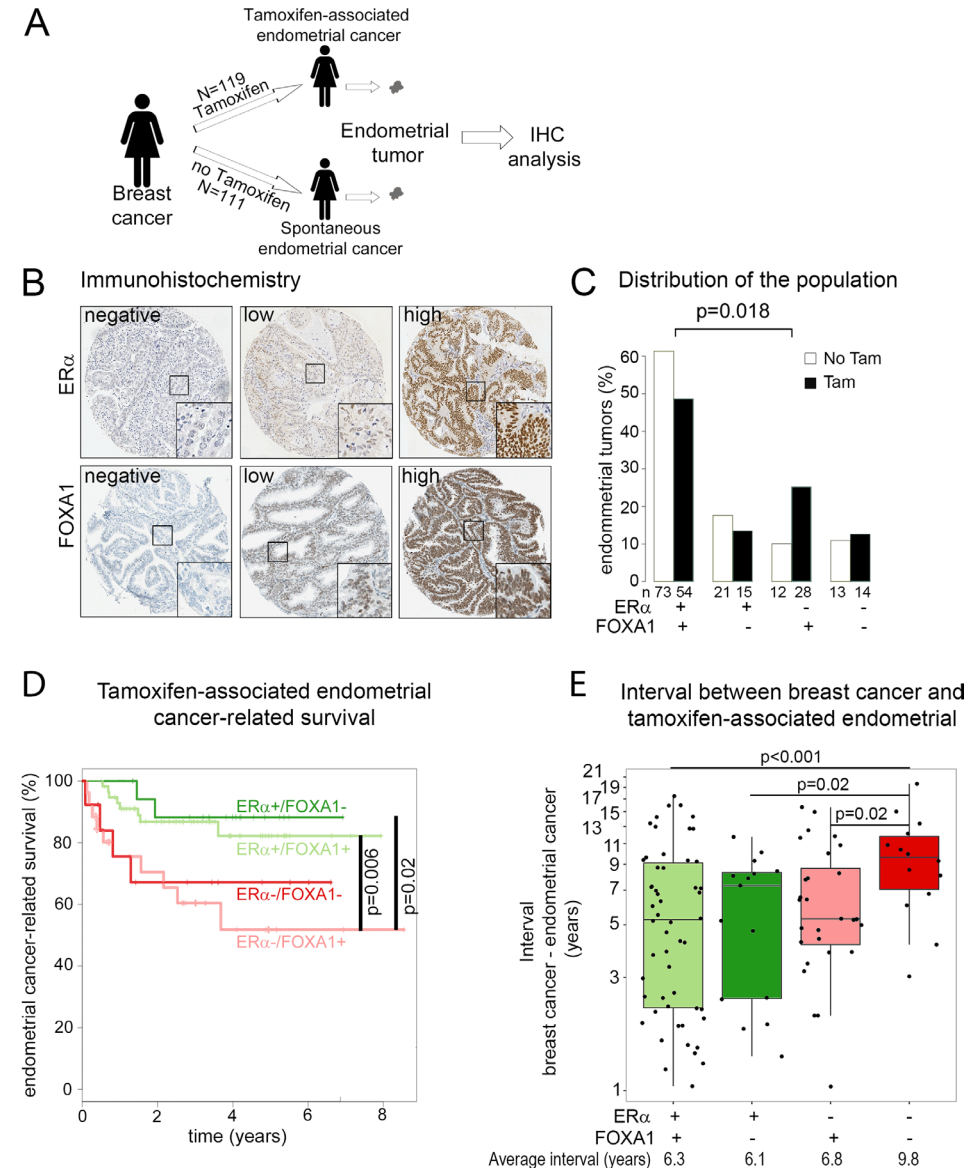


Figure 5. Immunohistochemistry analysis of FOXA1 and ER α in tamoxifen-associated endometrial cancer.

- A)** Overview of the study design. Endometrial tumor tissue was analyzed from patients who were previously treated for breast cancer. Half of these patients received tamoxifen for breast cancer treatment, while the other half did not receive any endocrine treatment.
- B)** Immunohistochemistry for ER α and FOXA1 showing no (left), low (middle), or high (right) protein expression.
- C)** Bar graph representing percentage and absolute numbers of patients that were categorized as ER α +/FOXA1+, ER α +/FOXA1-, ER α -/FOXA1+, or ER α -/FOXA1- and

tested for association with ER α and FOXA1 levels, as determined by immunohistochemistry (Figure 5B for example staining).

Scatter plot visualizations illustrated that FOXA1 and ER α positive cells in endometrial tumor specimens do not associate (Supplementary Figure S7), suggesting that ER α and FOXA1 expression levels may identify different patient groups. Therefore, tumors were categorized in groups that express only ER α , only FOXA1, both ER α and FOXA1, or neither. Most endometrial tumors are positive for both ER α and FOXA1, irrespective of treatment (Figure 5C). FOXA1⁺/ER α ⁻ tumors were enriched among tamoxifen-treated patients at the expense of the tumors that are positive for both ER α and FOXA1 (Fisher exact test: $P = 0.018$). ER α expression strongly associated with endometrial cancer patient survival, in agreement with previous immunohistochemical reports^{39,40}.

In contrast to previous reports^{33,34}, FOXA1 expression did not associate with survival of endometrial cancer patients, irrespective whether they did (Figure 5D) or did not receive tamoxifen (Supplementary Figure S8). Interestingly, tamoxifen-treated patients who developed an endometrial tumor had a shorter interval time between breast cancer and endometrial cancer when their endometrial tumor expressed ER α and/or FOXA1 (ER α : $P = 0.02$, FOXA1: $P = 0.02$; ER α /FOXA1: $P < 0.001$; Figure 5E). For patients who did not receive tamoxifen treatment for breast cancer, no significant differences in interval time between breast cancer and endometrial cancer diagnosis were found, based on ER α and FOXA1 levels in the endometrial tumor (Supplementary Figure S9).

Our data implicate a coordinated action between ER α and FOXA1, associated with a short interval time between breast cancer and endometrial cancer development in the tamoxifen-treated cases, without affecting endometrial cancer-related survival.

Discussion

Tamoxifen is a highly successful drug in the treatment of breast cancer. However, tamoxifen increases the risk of endometrial cancer. This direct link between breast cancer treatment and endometrial cancer development suggests a crucial role for ER α in both tumor types. Tamoxifen

grouped in tamoxifen-treated patients (white) and non-tamoxifen-treated patients (black). For statistics, Fisher exact test was used.

- D)** Endometrial cancer-specific survival of tamoxifen-treated patients, categorized as ER α ⁺/FOXA1⁺, ER α ⁺/FOXA1⁻, ER α ⁻/FOXA1⁺, or ER α ⁻/FOXA1⁻.
- E)** Box plot depicting interval time (years) between breast cancer diagnosis and endometrial cancer diagnosis for patients who received tamoxifen. P values were not corrected for multiple testing. Average interval time in years is shown.

has been reported in endometrial cells to stimulate the recruitment of coactivators to a subset of genes, similar to estrogen⁹. Between a breast cancer cell line and an endometrial cancer cell line, limited overlap of ER α sites was observed¹³, giving rise to differential gene expression between those cell lines following ligand treatment. More recently, the same lab reported shared ER α sites between these cell lines to be associated with strong EREs, inaccessible chromatin regions and lack of DNA methylation²⁹. In contrast, non-ERE-mediated ER α action was found dominant in tissue-type specific interactions, which co-occurred with other transcription factors and cell-type specific chromatin accessibility²⁹. This previous report was based on a single endometrial cancer cell line, while our study is the first to assess genomic behavior of ER α in several surgical specimens of endometrial cancer patients. We show a significant level of ER α overlap between breast cancer samples and endometrial cancer samples, being enriched for ESR1 and FOXA1 motifs. With this, our data illustrate that functional characterization of ER α genomic action can be accelerated by a joined analysis on cell line studied in conjunction with primary human tissue specimens.

Analogous to previous observations in breast cancer, endometrial ER α preferably binds enhancers, which were marked by H3K27ac and RNA polymerase II, suggesting that these enhancers are active. Furthermore, ER α binding events in endometrial tumor specimens are enriched for motifs of well-established transcriptional regulators in the field of breast cancer, including FOXA1¹⁵. FOXA1 was previously reported to be expressed in endometrial tissue, and downregulated in poorly differentiated endometrial cancer³² where low FOXA1 is associated with poor outcome^{33,34}. In line with these previous reports, we show that endometrial tumor cells express FOXA1, even though we do not observe an association of FOXA1 with clinical outcome in endometrial cancer in our cohort. Because patients in our cohort developed both breast cancer as well as endometrial cancer⁷, we may have enriched for patients with a genetic predisposition to developing both tumors types. Therefore, our study population may be intrinsically different from sporadic cases that only developed endometrial cancer³³. Here, we illustrate that FOXA1 chromatin binding sites are shared with ER α in tamoxifen-associated endometrial cancer. These sites are not exclusively bound by ER α or FOXA1, but are in fact regulated through a large multiprotein transcriptional network, jointly mediating ER α -driven gene profiles in endometrial cancer.

Multiple other proteins found to associate with breast cancer outcome have been implicated in endometrial cancer development, including PAX2^{10,12} and SRC1^{9,41}. Here, we show that FOXA1 can be added to this list, exposing a bivalent role in response to tamoxifen treatment, dependent on tissue type; while high FOXA1 expression is a favorable prognostic factor in breast cancer²¹, its expression levels associate with short interval

time between breast cancer diagnosis and tamoxifen-associated endometrial cancer development without affecting outcome in this cohort. This closely follows parallel observations made for PAX2, and validates inverse relations of transcriptional regulators between breast and endometrial cancer with respect to tumorigenesis and response to endocrine agents.

To conclude, we show that endometrial tumor cells express FOXA1, serving the classical ER α -pioneer factor role as was originally identified in breast cancer¹⁵. Yet, instead of facilitating the inhibitory potential of tamoxifen on ER α activity, FOXA1 may enable receptor activation through tamoxifen in endometrial tissue in postmenopausal women. This function of FOXA1 has far-reaching consequences, where it may dictate the stimulatory effects of tamoxifen treatment on endometrial cancer development.

Acknowledgments

The authors thank Ron Kerkhoven, Shan Baban, and Marja Nieuwland from the NKI genomics facility for sample processing and Arno Velds for bioinformatics support. They acknowledge the NKI-AVL Core Facility Molecular Pathology & Biobanking (CFMPB) for supplying NKI-AVL Biobank material and lab support. The authors thank Joyce Sanders for help with pathological analyses and Jos Jonkers and Jason Carroll for critically reading the manuscript and valuable suggestions. This work was supported by grants from the Dutch Cancer Society and Pink Ribbon.

References

1. Shiau AK, Barstad D, Loria PM, Cheng L, Kushner PJ, Agard DA, et al. The structural basis of estrogen receptor/coactivator recognition and the antagonism of this interaction by tamoxifen. *Cell* 1998;95:927-37.
2. van Leeuwen FE, Benraadt J, Coebergh JW, Kiemeny LA, Gimbire CH, Otter R, et al. Risk of endometrial cancer after tamoxifen treatment of breast cancer. *Lancet* 1994;343:448-52.
3. Bernstein L, Deapen D, Cerhan JR, Schwartz SM, Liff J, McGann-Maloney E, et al. Tamoxifen therapy for breast cancer and endometrial cancer risk. *Journal of the National Cancer Institute* 1999;91:1654-62.
4. Swerdlow AJ, Jones ME. Tamoxifen treatment for breast cancer and risk of endometrial cancer: a case-control study. *Journal of the National Cancer Institute* 2005;97:375-84.
5. Bergman L, Beelen ML, Gallee MP, Hollema H, Benraadt J, van Leeuwen FE. Risk and prognosis of endometrial cancer after tamoxifen for breast cancer. Comprehensive Cancer Centres' ALERT Group. Assessment of Liver and Endometrial cancer Risk following Tamoxifen. *Lancet* 2000;356:881-7.
6. Curtis RE, Freedman DM, Sherman ME, Fraumeni JF, Jr. Risk of malignant mixed mullerian tumors after tamoxifen therapy for breast cancer. *Journal of the National Cancer Institute* 2004;96:70-4.

7. Hoogendoorn WE, Hollema H, van Boven HH, Bergman E, de Leeuw-Mantel G, Platteel I, et al. Prognosis of uterine corpus cancer after tamoxifen treatment for breast cancer. *Breast cancer research and treatment* 2008;112:99-108.
8. Jones ME, van Leeuwen FE, Hoogendoorn WE, Mourits MJ, Hollema H, van Boven H, et al. Endometrial cancer survival after breast cancer in relation to tamoxifen treatment: pooled results from three countries. *Breast cancer research* : BCR 2012;14:R91.
9. Shang Y, Brown M. Molecular determinants for the tissue specificity of SERMs. *Science* 2002;295:2465-8.
10. Wu H, Chen Y, Liang J, Shi B, Wu G, Zhang Y, et al. Hypomethylation-linked activation of PAX2 mediates tamoxifen-stimulated endometrial carcinogenesis. *Nature* 2005;438:981-7.
11. Michalides R, Griekspoor A, Balkenende A, Verwoerd D, Janssen L, Jalink K, et al. Tamoxifen resistance by a conformational arrest of the estrogen receptor alpha after PKA activation in breast cancer. *Cancer cell* 2004;5:597-605.
12. Hurtado A, Holmes KA, Geistlinger TR, Hutcheson IR, Nicholson RI, Brown M, et al. Regulation of ERBB2 by oestrogen receptor-PAX2 determines response to tamoxifen. *Nature* 2008;456:663-6.
13. Gertz J, Reddy TE, Varley KE, Garabedian MJ, Myers RM. Genistein and bisphenol A exposure cause estrogen receptor 1 to bind thousands of sites in a cell type-specific manner. *Genome research* 2012;22:2153-62.
14. Hurtado A, Holmes KA, Ross-Innes CS, Schmidt D, Carroll JS. FOXA1 is a key determinant of estrogen receptor function and endocrine response. *Nature genetics* 2011;43:27-33.
15. Carroll JS, Liu XS, Brodsky AS, Li W, Meyer CA, Szary AJ, et al. Chromosome-wide mapping of estrogen receptor binding reveals long-range regulation requiring the forkhead protein FoxA1. *Cell* 2005;122:33-43.
16. Laganier J, Deblois G, Lefebvre C, Bataille AR, Robert F, Giguere V. From the Cover: Location analysis of estrogen receptor alpha target promoters reveals that FOXA1 defines a domain of the estrogen response. *Proceedings of the National Academy of Sciences of the United States of America* 2005;102:11651-6.
17. Sorlie T, Perou CM, Tibshirani R, Aas T, Geisler S, Johnsen H, et al. Gene expression patterns of breast carcinomas distinguish tumor subclasses with clinical implications. *Proceedings of the National Academy of Sciences of the United States of America* 2001;98:10869-74.
18. Perou CM, Sorlie T, Eisen MB, van de Rijn M, Jeffrey SS, Rees CA, et al. Molecular portraits of human breast tumours. *Nature* 2000;406:747-52.
19. Ademuyiwa FO, Thorat MA, Jain RK, Nakshatri H, Badve S. Expression of Forkhead-box protein A1, a marker of luminal A type breast cancer, parallels low Oncotype DX 21-gene recurrence scores. *Modern pathology* : an official journal of the United States and Canadian Academy of Pathology, Inc 2010;23:270-5.

20. Thorat MA, Marchio C, Morimiya A, Savage K, Nakshatri H, Reis-Filho JS, et al. Forkhead box A1 expression in breast cancer is associated with luminal subtype and good prognosis. *Journal of clinical pathology* 2008;61:327-32.
21. Badve S, Turbin D, Thorat MA, Morimiya A, Nielsen TO, Perou CM, et al. FOXA1 expression in breast cancer--correlation with luminal subtype A and survival. *Clinical cancer research : an official journal of the American Association for Cancer Research* 2007;13:4415-21.
22. Kong SL, Li G, Loh SL, Sung WK, Liu ET. Cellular reprogramming by the conjoint action of ERalpha, FOXA1, and GATA3 to a ligand-inducible growth state. *Molecular systems biology* 2011;7:526.
23. Fles R, Hoogendoorn WE, Platteel I, Scheerman CE, de Leeuw-Mantel G, Mourits MJ, et al. Genomic profile of endometrial tumors depends on morphological subtype, not on tamoxifen exposure. *Genes, chromosomes & cancer* 2010;49:699-710.
24. Zwart W, Theodorou V, Kok M, Canisius S, Linn S, Carroll JS. Oestrogen receptor-co-factor-chromatin specificity in the transcriptional regulation of breast cancer. *The EMBO journal* 2011;30:4764-76.
25. Jansen MP, Knijnenburg T, Reijm EA, Simon I, Kerkhoven R, Droog M, et al. Hallmarks of aromatase inhibitor drug resistance revealed by epigenetic profiling in breast cancer. *Cancer research* 2013;73:6632-41.
26. Schmidt D, Wilson MD, Spyrou C, Brown GD, Hadfield J, Odom DT. ChIP-seq: using high-throughput sequencing to discover protein-DNA interactions. *Methods* 2009;48:240-8.
27. Kumar V, Muratani M, Rayan NA, Kraus P, Lufkin T, Ng HH, et al. Uniform, optimal signal processing of mapped deep-sequencing data. *Nature biotechnology* 2013;31:615-22.
28. Zhang Y, Liu T, Meyer CA, Eeckhoutte J, Johnson DS, Bernstein BE, et al. Model-based analysis of ChIP-Seq (MACS). *Genome biology* 2008;9:R137.
29. Gertz J, Savic D, Varley KE, Partridge EC, Safi A, Jain P, et al. Distinct properties of cell-type-specific and shared transcription factor binding sites. *Molecular cell* 2013;52:25-36.
30. Ross-Innes CS, Stark R, Teschendorff AE, Holmes KA, Ali HR, Dunning MJ, et al. Differential oestrogen receptor binding is associated with clinical outcome in breast cancer. *Nature* 2012;481:389-93.
31. Wolf I, Bose S, Williamson EA, Miller CW, Karlan BY, Koeffler HP. FOXA1: Growth inhibitor and a favorable prognostic factor in human breast cancer. *International journal of cancer Journal international du cancer* 2007;120:1013-22.
32. Wang J, Bao W, Qiu M, Liao Y, Che Q, Yang T, et al. Forkhead-box A1 suppresses the progression of endometrial cancer via crosstalk with estrogen receptor alpha. *Oncology reports* 2014;31:1225-34.
33. Tangen IL, Krakstad C, Halle MK, Werner HM, Oyan AM, Kusonmano K, et al. Switch in FOXA1 status associates with endometrial cancer progression. *PloS one* 2014;9:e98069.
34. Abe Y, Ijichi N, Ikeda K, Kayano H, Horie-Inoue K, Takeda S, et al. Forkhead box transcription factor, forkhead box A1, shows negative association with

- lymph node status in endometrial cancer, and represses cell proliferation and migration of endometrial cancer cells. *Cancer science* 2012;103:806-12.
35. Qiu M, Bao W, Wang J, Yang T, He X, Liao Y, et al. FOXA1 promotes tumor cell proliferation through AR involving the Notch pathway in endometrial cancer. *BMC cancer* 2014;14:78.
 36. Kleine W, Maier T, Geyer H, Pfeiderer A. Estrogen and progesterone receptors in endometrial cancer and their prognostic relevance. *Gynecologic oncology* 1990;38:59-65.
 37. Risinger JI, Allard J, Chandran U, Day R, Chandramouli GV, Miller C, et al. Gene expression analysis of early stage endometrial cancers reveals unique transcripts associated with grade and histology but not depth of invasion. *Frontiers in oncology* 2013;3:139.
 38. Huang YW, Kuo CT, Chen JH, Goodfellow PJ, Huang TH, Rader JS, et al. Hypermethylation of miR-203 in endometrial carcinomas. *Gynecologic oncology* 2014;133:340-5.
 39. Mylonas I. Prognostic significance and clinical importance of estrogen receptor alpha and beta in human endometrioid adenocarcinomas. *Oncology reports* 2010;24:385-93.
 40. Shabani N, Kuhn C, Kunze S, Schulze S, Mayr D, Dian D, et al. Prognostic significance of oestrogen receptor alpha (ERalpha) and beta (ERbeta), progesterone receptor A (PR-A) and B (PR-B) in endometrial carcinomas. *European journal of cancer* 2007;43:2434-44.
 41. Redmond AM, Bane FT, Stafford AT, McIlroy M, Dillon MF, Crotty TB, et al. Coassociation of estrogen receptor and p160 proteins predicts resistance to endocrine treatment; SRC-1 is an independent predictor of breast cancer recurrence. *Clinical cancer research : an official journal of the American Association for Cancer Research* 2009;15:2098-106.

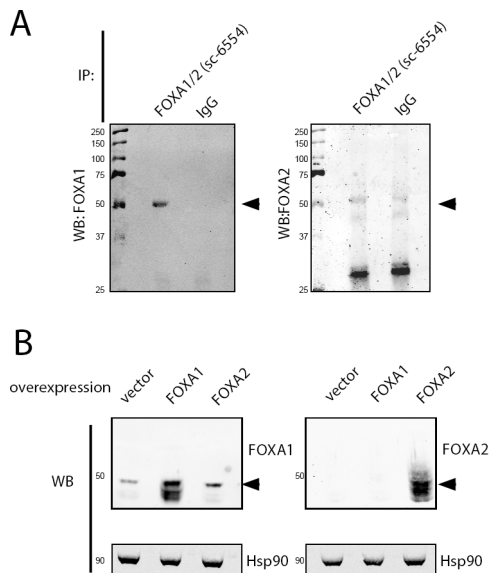
Supplementary Methods

Data Visualization, Motif Analysis and Genomic Distributions of Binding Events

ChIP-seq data snapshots were generated using the Integrative Genome Viewer IGV 2.1 (www.broadinstitute.org/igv/). The genomic distributions of binding sites were analyzed using the cis-regulatory element annotation system (CEAS)¹. The genes closest to the binding site on both strands were analyzed. If the binding region is within a gene, CEAS software indicates whether it is in a 5'UTR, 3'UTR, coding exon, or intron. Promoter is defined as up to and including 3kb upstream from RefSeq 5' start. If a binding site is >3kb away from the RefSeq transcription start site, it is considered distal intergenic. Motif analyses were performed through the Cistrome (cistrome.org), applying the SeqPos motif tool². For motif analyses, an equal number of genomic regions were analyzed for the different conditions, and enriched motifs were identified for each of the peak subsets according to p-value with cutoffs indicated in the figure legends. RNA-seq data for Ishikawa cells, with and without estradiol treatment, is obtained from Encyclopedia of DNA Elements³ (for GEO accession number, see Supplementary Table S4). The cut-off used for gene expression was set at Fragments Per Kilo-base of exon per Million fragments mapped (FPKM) > 1 in two replicates. To compare binding sites of FOXA1 and ER α with other transcription factors in Ishikawa cell line, we obtained 22 ChIP-seq datasets for Ishikawa from the Encyclopedia of DNA Elements³ (Supplementary Table S4). To identify ER α and FOXA1 binding sites, only peaks conserved between both replicates were considered. For overlap between factors, Pearson correlation coefficients were measured using the `dba.overlap` function of the DiffBind package⁴. A network model was constructed using Ingenuity Pathway Analysis (IPA) to delineate cooperative and differential gene regulation, where all genes with a binding event of ER α and FOXA1 in the gene body or within 20kb upstream of the transcription start site were considered. The FPKM fold-change upon estradiol treatment of the genes is taken into account for constructing the network model. Given a set of genes, IPA infers 1) network models that maximally include the genes in the set and known interactions between them; 2) canonical pathways significantly associated to the set of genes; and 3) potential upstream regulators of the genes.

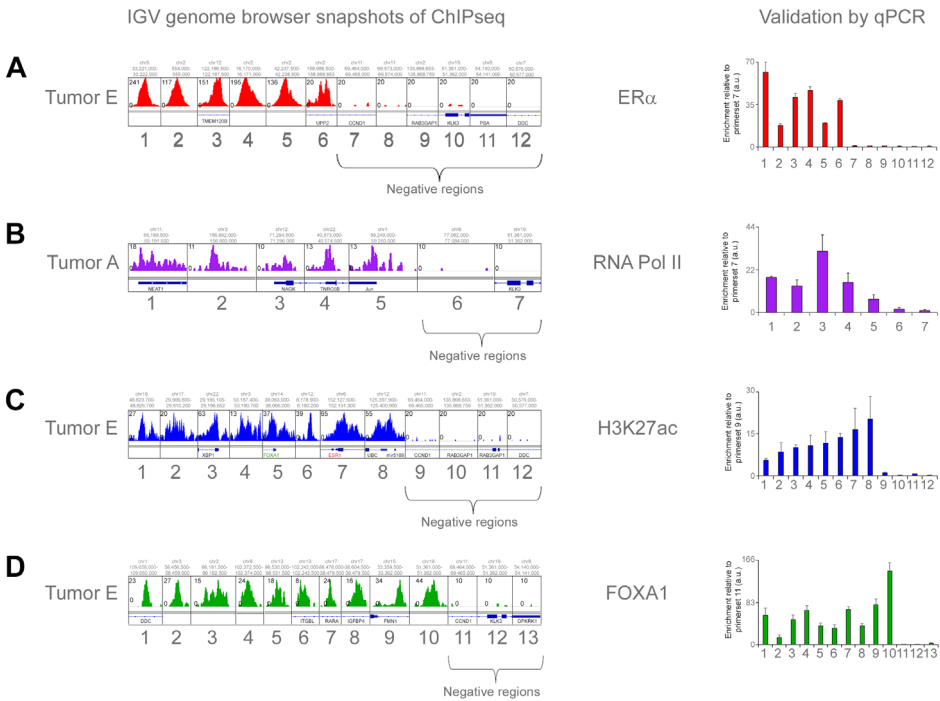
Supplementary References

1. Ji X, Li W, Song J, Wei L, Liu XS. CEAS: cis-regulatory element annotation system. *Nucleic acids research* 2006;34:W551-4.
2. He HH, Meyer CA, Shin H, Bailey ST, Wei G, Wang Q, et al. Nucleosome dynamics define transcriptional enhancers. *Nature genetics* 2010;42:343-7.
3. Consortium EP. The ENCODE (ENCyclopedia Of DNA Elements) Project. *Science* 2004;306:636-40.
4. Ross-Innes CS, Stark R, Teschendorff AE, Holmes KA, Ali HR, Dunning MJ, et al. Differential oestrogen receptor binding is associated with clinical outcome in breast cancer. *Nature* 2012;481:389-93.



Supplementary Figure S1.

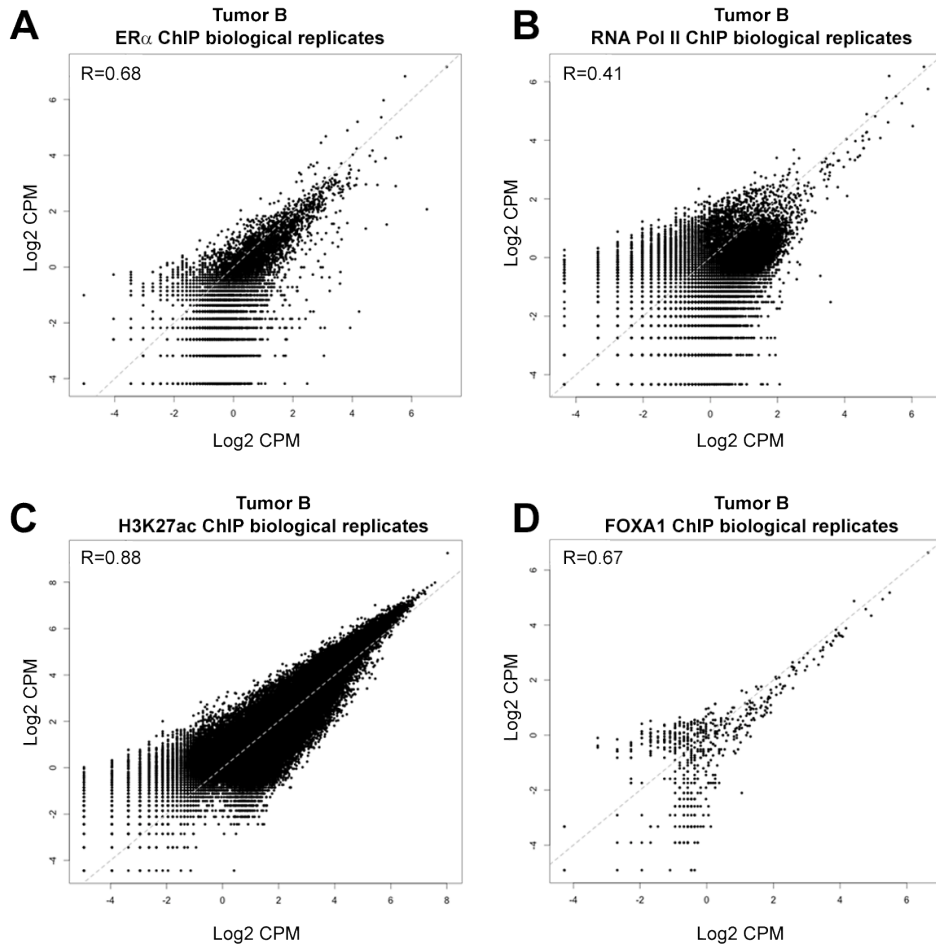
Validation of two FOXA1 antibodies that were used for either ChIP or Western blot. A, FOXA1/2(sc-6554) and the control IgG antibodies were used for an immunoprecipitation in MCF-7 cells. Western blot depicts immunoprecipitated fractions with specific antibodies raised for either FOXA1 (WMAB-2F83) or FOXA2 (WMAB-1200). B, Western blots, depicting transient overexpression of an empty vector, FOXA1 and FOXA2 in MCF-7 cells. The left blot was stained for FOXA1 (WMAB-2F83) and the right blot (WMAB-1200) for FOXA2. HSP90 was used as a loading control.



Supplementary Figure S2.

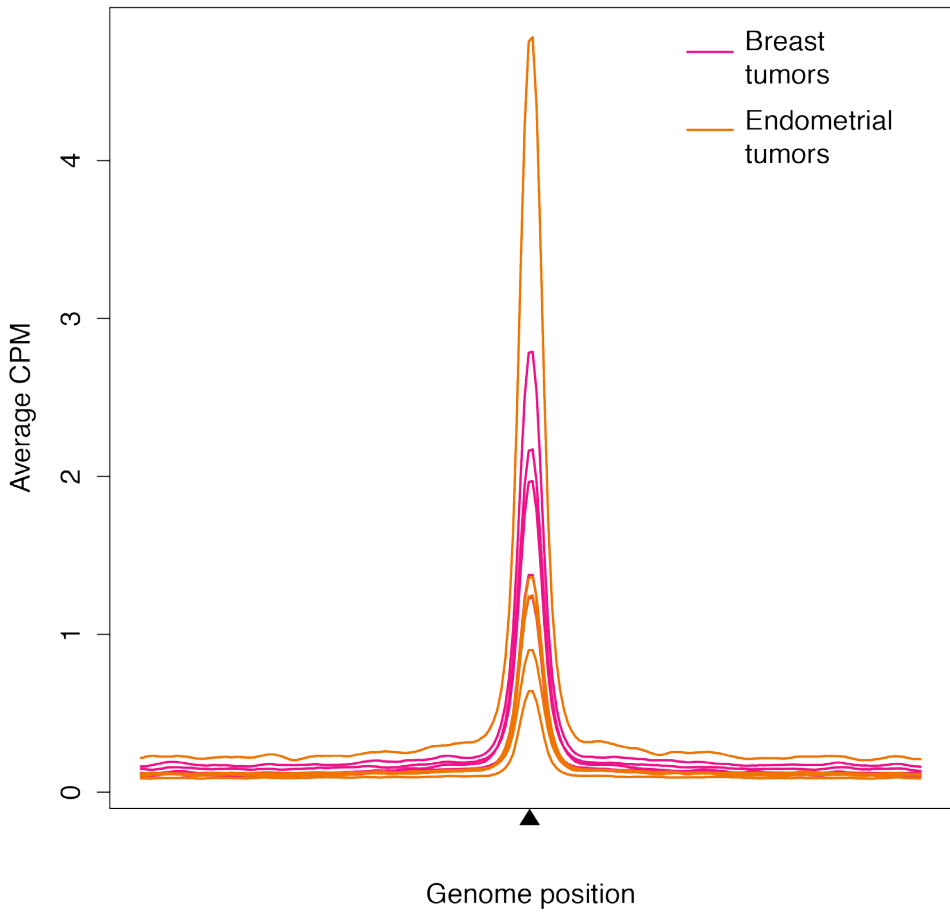
ChIP-QPCR validation of ChIP-seq peaks found in endometrial cancer specimens. ChIP-QPCR analyses were performed for both positive and negative regions, as identified through ChIP-seq, to validate binding sites identified for ERα (A), RNA Polymerase II (B), H3K27Ac (C) and FOXA1 (D). Left: Genome browser snapshots for the positive and negative regions. Tag count and genomic coordinates are indicated. Right: ChIP-QPCR analyses for the same binding sites. Data are normalized over negative region as indicated on the y-axis. Error bars indicate SD values from triplicate measurements. Corresponding primers can be found in supplementary table S3.

Scatter plots of the reads in the union of peaks between the replicates (log-normalized values)



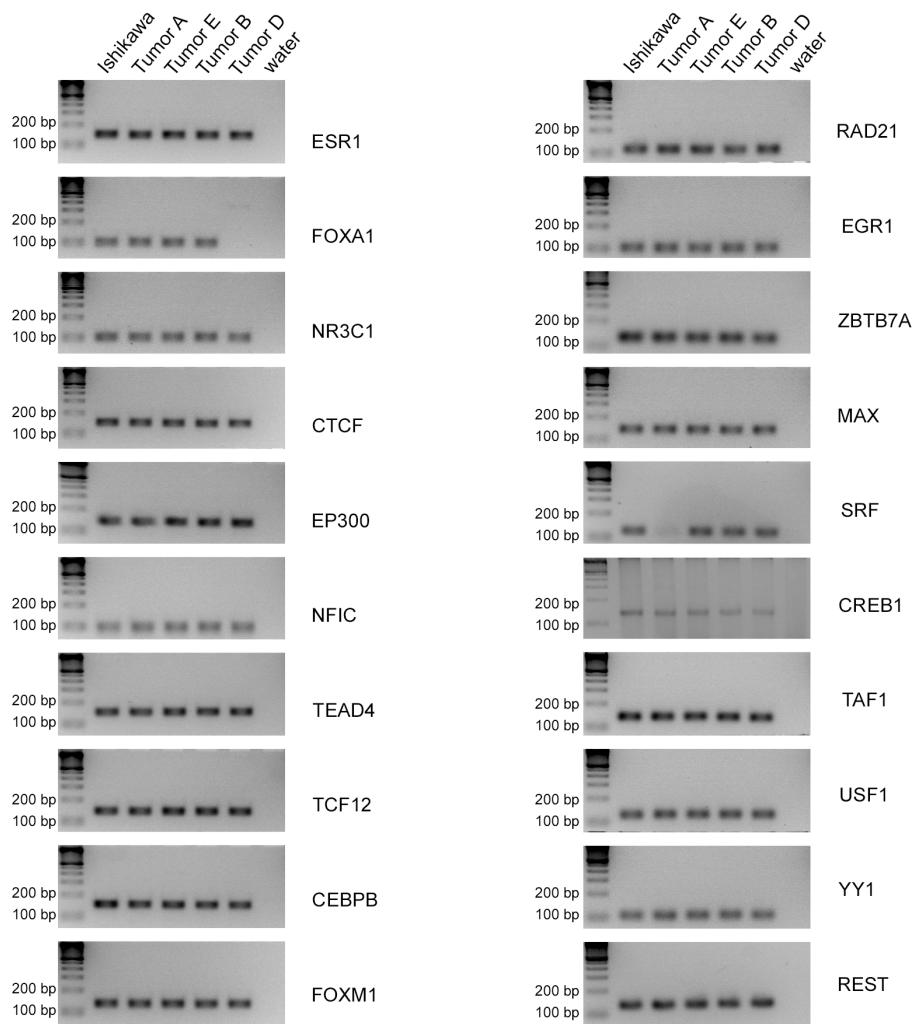
Supplementary Figure S3.

Biological replicates of ChIP-seq analyses for ER α (A), RNA Polymerase II (B), H3K27Ac (C) and FOXA1 (D). Scatterplot indicates correlation of the read counts for the identified peaks in the two replicates for each factor. Pearson correlation coefficients are shown.

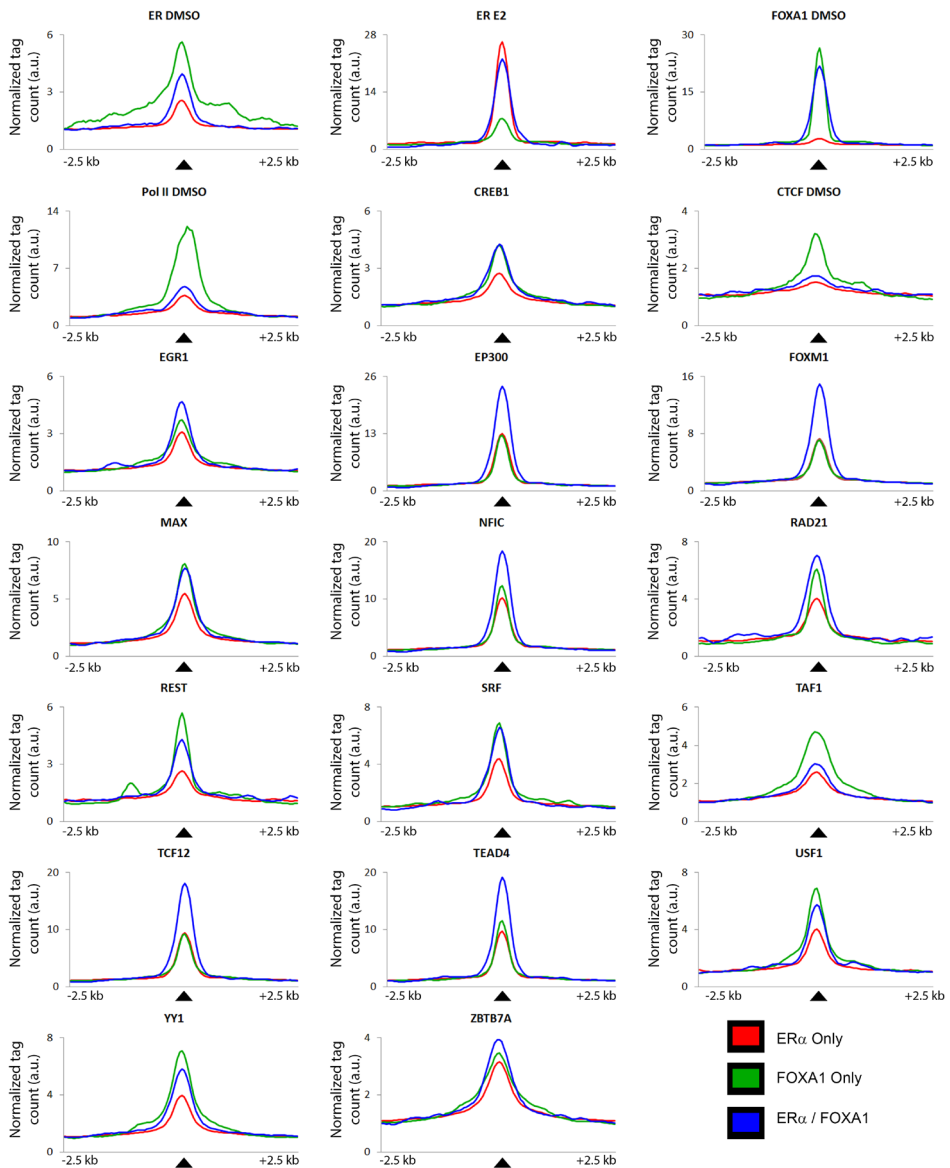


Supplementary Figure S4.

Average normalized ER α ChIP-seq signal of endometrial and breast cancer specimens. Counts per Million (CPM)-normalized average read count of ChIP-seq data visualized in Figure 2D. Data was centered on the peak regions and includes a 5 kb window around the peak. Y-axis shows normalized read count.

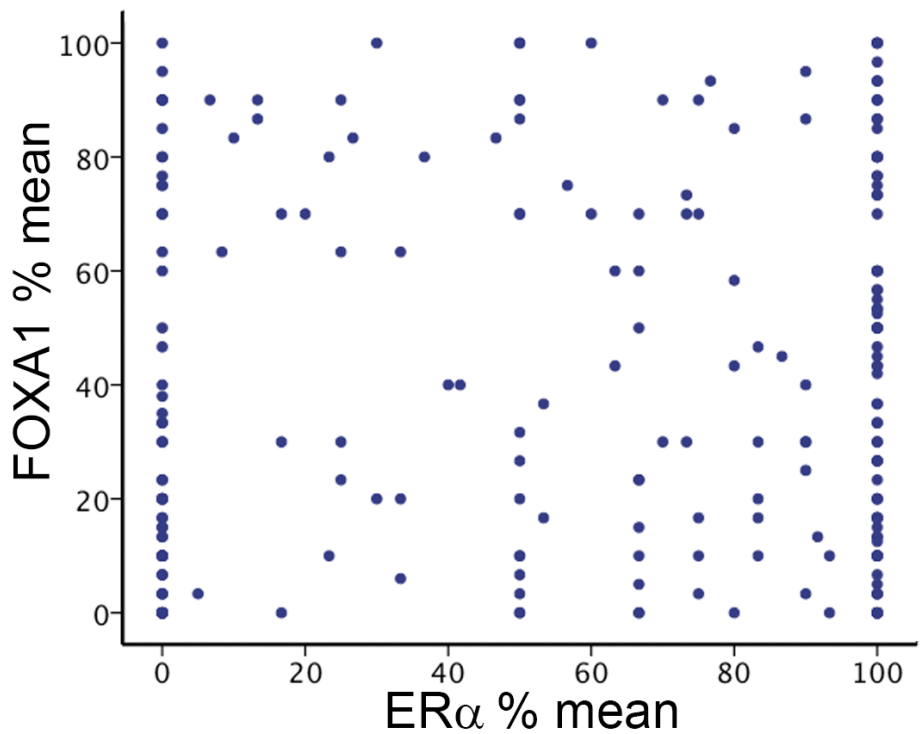


Supplementary Figure S5. RT-PCR analysis of 20 transcription factors in four tamoxifen-associated endometrial tumors and Ishikawa cells. Corresponding primers can be found in supplementary table S6.

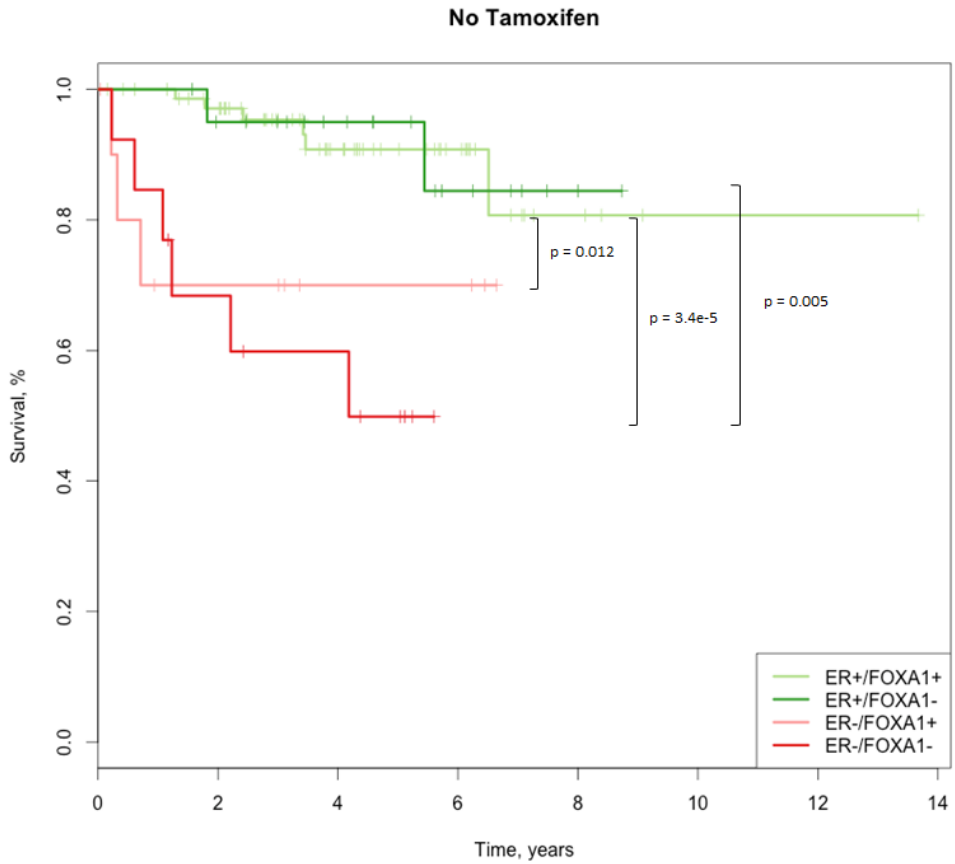


Supplementary Figure S6.

2D graph, showing normalized read count of the shared binding sites for ER α and FOXA1 (blue), ER α only (red) and FOXA1 only (green) in ChIP-seq datasets of all indicated transcriptional regulators in the endometrial cancer cell line Ishikawa (ENCODE, see Supplementary table S4). Data are centered on the top of the peak regions, depicting a 5 kb window around the peak. Y-axis shows read count.

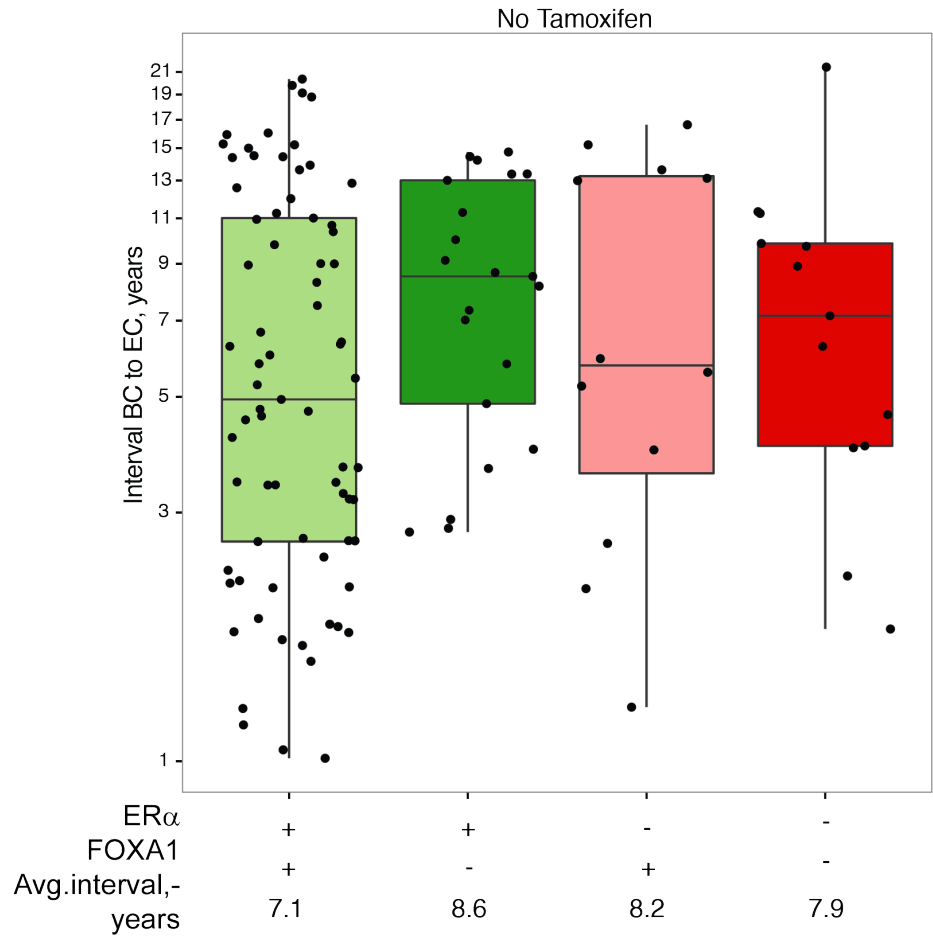


Supplementary Figure S7. Scatter plot showing the relationship between ER α (X-axis) and FOXA1 (Y-axis) staining. Mean % of positive tumor cells is shown, where each dot indicates one tumor sample. Pearson correlation coefficient is 0.081, $p=0.308$.



Supplementary Figure S8.

Kaplan-Meier survival plot of endometrial cancer patients who were not treated with tamoxifen for their breast cancer, categorized as ER α +/FOXA1+, ER α +/FOXA1-, ER α -/FOXA1+ or ER α -/FOXA1-.



Supplementary Figure S9.
Box plot, depicting interval time (years) between breast cancer diagnosis and endometrial cancer diagnosis for patients who did not receive tamoxifen. P values were not corrected for multiple testing. Average interval time in years is shown. MC-UC = interval between breast cancer and endometrial cancer.

Supplementary Table S1: Clinicopathological parameters.

	tamoxifen (n=111)		No tamoxifen (n = 119)	
Interval between diagnosis of breast and uterine cancer [months]				
<24	14	12.6%	14	11.8%
24-36	13	11.7%	16	13.4%
36-60	18	16.2%	22	18.5%
60-120	42	37.8%	29	24.4%
>120	24	21.6%	38	31.9%
Age at diagnosis of breast cancer [years]				
<55	22	19.8%	34	28.6%
55-64	38	34.2%	34	28.6%
65-74	30	27.0%	39	32.8%
>75	21	18.9%	12	10.1%
Age at diagnosis of endometrial cancer				
<65	33	29.7%	38	31.9%
65-74	34	30.6%	45	37.8%
>75	44	39.6%	36	30.3%
Histological type				
Endometrioid adenocarcinoma	83	74.8%	100	84.0%
clear cell and serous adenocarcinoma	14	12.6%	9	7.6%
Carcinosarcoma	6	5.4%	6	5.0%
Sarcoma	8	7.2%	4	3.4%
Grade (endometrioid adenocarcinomas only)				
1	51	45.9%	63	52.9%
2	18	16.2%	23	19.3%
3	12	10.8%	14	11.8%
missing	2	1.8%	0	0.0%
FIGO stage				
I	81	73.0%	93	78.2%
II	15	13.5%	14	11.8%
III	10	9.0%	5	4.2%
IV	4	3.6%	6	5.0%
missing	1	0.9%	1	0.8%

Supplementary Table S2: Patient characteristics of endometrioid adenocarcinomas used for ChIP-seq.

Tumor	Figo Stage	Tamoxifen (yrs)	MC-UC (yrs)	Age UC (yrs)	Number of peaks per ChIP				Tamoxifen status	
					ER α	RNA Pol II	H3K27ac	FOXA1	at surgery	Tumor (%)
A	I	5.59	6.37	76.44	1422	1780	36469	706	User	70
B	I	3.16	3.18	69.20	6750	13720	30619	384	User	60
C	I	5.26	5.03	60.35	6242	159	31461	352	Stopped 1-2 months	75
D	I	2.70	3.43	54.46	18636	7143	N/A	N/A	User	70
E	I	4.18	4.65	55.78	25023	198	28272	6811	User	60
Biological replicate B					2242	7376	40791	292		

Supplementary Table S3: Primer sequences for ChIP-qPCR
Corresponds with Supplementary Figure S2.

	Primer pair	Sequences
Positive control	ER α #1	TGGCCCTAAATGTGCTGCT (FWD) TTTGGCCTCTTCCTCTCTCT (REV)
	ER α #2	CCTTCTCTCTGGGGGTGA (FWD) GCACCACCAACACTCACATT (REV)
	ER α #3	TGATGTCATTGCCACCTTGT (FWD) AACAGGGTCAGGGTGAAGT (REV)
	ER α #4	CTGGGGGAACCTTCAATTTT (FWD) GTGAGAACACTGCGAGGTCA (REV)
	ER α #5	CCCAGGTCACTGCAATCTTT (FWD) CCTGGTCCAGACCACAGAAT (REV)
	ER α #6	ATATTTGCCGAGCTCAAGT (FWD) CCTGAGCTAGCACATGGTGA (REV)
	RNA Pol II #1	GGGACAGACAGGAGAGATG (FWD) ACTGTGGTCCCCCTAGACCT (REV)
	RNA Pol II #2	TTGATTTCACAACGGTCGAG (FWD) GAGACTCGGATTTCGCGATT (REV)
	RNA Pol II #3	GTCCATCTCTGGAAGCAGGA (FWD) CGTCCCTCAGGCTGTCTTC (REV)
	RNA Pol II #4	CCCCTTTCCTGATTGACAAA (FWD) GGCCATTTTGGCTTGAAGTA (REV)
	RNA Pol II #5	CCCCTAAAAATAGCCCATGA (FWD) CATTACCTCATCCCGTGAGC (REV)
	H3K27ac #1	GTCGAGGCTGAGGTCTCACT (FWD) AGCTTAAGACCGGCACCTCT (REV)
	H3K27ac #2	GTACTCCTCCGCTCCTTCT (FWD) TACAGCATGTGCTTTTCTG (REV)
	H3K27ac #3	TCTCTGGGCTGGCACCAT (FWD) GCGGTGCGTAGCTGGAG (REV)
	H3K27ac #4	TCAGAAATCCAGCCTTCTC (FWD) GCAGTAATGGTGAGGCCTTG (REV)
	H3K27ac #5	GCGTGTCTGCGTAGTAGTG (FWD) AGGGCTGGATGGTTGTATTG (REV)
	H3K27ac #6	GGACGTGCTCTTATCCCTGA (FWD) GACGCACTGAATGGAAAGGT (REV)
	H3K27ac #7	ATGACCATGACCCTCCACAC (FWD) TTGCTGCTGCCAGGTACAC (REV)
	H3K27ac #8	GTAATGACGGGGCTTCCTTT (FWD) TGAGATCTGCCGAGTCATTG (REV)
	FOXA1 #1	ACCCACCCTCTTCTCTGTT (FWD) TGTTCAATGGCCACTGTTTG (REV)
	FOXA1 #2	CCTAGCTGCAACCCAAATC (FWD) GCAATAGAGGGAATGAAGGA (REV)
	FOXA1 #3	CATTATGCCCTCCCCTCT (FWD) GAAACCGATCTATGGGCTGA (REV)
	FOXA1 #4	CAGCCGTCTTGCAAGAAA (FWD) GCCGAGGAACACTGAAAGAC (REV)
	FOXA1 #5	TGCCTGGGATACCAAGGTTA (FWD) CTGGTTGCTCTCTTGAGCTT (REV)
	FOXA1 #6	CGCAAATGTCAGCATGTTCT (FWD) TTGTTTCACAGAGCCAATG (REV)
	FOXA1 #7	CTTGAGGTCAGGCAGTCTCC (FWD) AAGCCACTCCAAGGTAGGTG (REV)
	FOXA1 #8	GGCTCTTCAGTCTGCCAGTT (FWD) CACGCTGACTTCAACAGCTT (REV)
	FOXA1 #9	AGGGATAACCCACACGACTG (FWD) AGCCTGGGCTGTTTACTCTG (REV)
	FOXA1 #10	CACCACTGTTAGGCTGCAAA (FWD) TCCTTCCCATTCTTTCCAA (REV)
Negative control	ER α #7 H3K27ac #9 FOXA1 #11	TGCCACACACCAAGTACTTT (FWD), ACAGCCAGAAGCTCCAAAAA (REV)
	ER α #8	TGGCCCTTGATACTGGAGTC (FWD), GACATCCAAGGCAAGATGGT (REV)
	ER α #9 H3K27ac #10	CTAGGAGGGTGGAGGTAGGG (FWD) GCCCAACACAGGAGTAATGA (REV)
	ER α #10 Pol #7 H3K27ac #11 FOXA1 #12	CACACCCGCTCTACGATATGA (FWD) GAGCTCGGCAGGCTCTGA (REV)
	ER α #11 FOXA1 #13	CTGCTCCTGGCATTATCCTC (FWD) TGTGGCTCTCAGCAGGAAGT (REV)
	ER α #12 H3K27ac #12	AATCCTTTGGCTGCCAGTTA (FWD) AGGTACTTCTGGGCATGGT (REV)
	Pol #6	AGACTCCAGACGCACCATCT (FWD) GGGTGACTTTGTGTCCGAAA (REV)

Supplementary Table S4: Accession numbers of Ishikawa RNA-seq and ChIP-seq datasets generated by the ENCODE consortium and publicly available ER α ChIP-seq data from breast tumors.

Cell line/tissue		Accession number
RNA-seq Ishikawa		GSE35584
Ishikawa	DMSO	GSM923423
Ishikawa	E2	GSM923427
ChIP-seq Ishikawa		GSE32465
Ishikawa	EGR1	GSM1010888
Ishikawa	USF1	GSM1010886
Ishikawa	TEAD4	GSM1010885
Ishikawa	CREB1	GSM1010857
Ishikawa	FOXM1	GSM1010856
Ishikawa	NFIC	GSM1010855
Ishikawa	TCF12	GSM1010842
Ishikawa	REST/NRSF	GSM1010841
Ishikawa	MAX	GSM1010807
Ishikawa	CEBPB	GSM1010802
Ishikawa	RAD21	GSM1010801
Ishikawa	CTCF	GSM1010774
Ishikawa	SRF	GSM1010762
Ishikawa	p300	GSM1010759
Ishikawa	YY1	GSM1010753
Ishikawa	ZBTB7A	GSM1010752
Ishikawa	TAF1	GSM1010733
Ishikawa	RNA Pol II	GSM803536
Ishikawa	GR (EtOH)	GSM803464
Ishikawa	GR (DEX)	GSM803340
Ishikawa	FOXA1	GSM803444
Ishikawa	ER α (E2)	GSM803422
Ishikawa	ER α (DMSO)	GSM803421
ChIP-seq Breast tumors		GSE40867
Breast tumor 1	ER α	GSM1003720
Breast tumor 2	ER α	GSM1003734
Breast tumor 3	ER α	GSM1003723
Breast tumor 4	ER α	GSM1003717
Breast tumor 5	ER α	GSM1003714

Supplementary Table S5: Patient characteristics of breast tumors used in Figure 2.

Sample	Age at diagnosis	Tumor type	Tumor Grade	PR.status	HER2.status
1	76	IDC	1	positive	N/A
2	58	IDC	N/A	positive	N/A
3	71	IDC	2	positive	negative
4	51	IDC	3	positive	negative
5	69	IDC	2	positive	negative

N/A = Not Available

Supplementary Table S6: ChIP-seq read count and mapped reads of endometrial tumors.

cell line/ tissue	ChIP Ab	read count	mapped reads	% mapped
Tumor A	ER α	15331544	14207826	92.7
Tumor A	RNA Pol II	23862573	21681488	90.9
Tumor A	H3K27ac	23175814	22016196	95.0
Tumor A	FOXA1	20609022	19267411	93.5
Tumor B	ER α	24549638	23652264	96.3
Tumor B	RNA Pol II	32192458	20334325	63.2
Tumor B	H3K27ac	23110704	22653542	98.0
Tumor B	FOXA1	21130957	19291797	91.3
Tumor C	ER α	21716690	20774510	95.7
Tumor C	RNA Pol II	16224209	15248669	94.0
Tumor C	H3K27ac	25380006	23402591	92.2
Tumor C	FOXA1	23378746	22458122	96.1
Tumor D	ER α	19603948	17976811	91.7
Tumor D	RNA Pol II	25018163	23111684	92.4
Tumor E	ER α	14930170	12101826	81.1
Tumor E	RNA Pol II	19557143	10884677	55.7
Tumor E	H3K27ac	20390107	19103140	93.7
Tumor E	FOXA1	15259727	13819149	90.6
Tumor input		22580567	21760992	96.4
Biological replicate B	ER α	19287976	18138678	94.0
Biological replicate B	RNA Pol II	21358572	20065872	94.0
Biological replicate B	H3K27ac	23442310	21669423	92.4
Biological replicate B	FOXA1	31834682	30078757	94.4

Supplementary Table S7: mRNA primer sequences
Primers correspond with Supplementary Figure S5.

Primer Sequences	
ESR1	TGGAGATCTTCGACATGCTG (FWD), TCCAGAGACTTCAGGGTGCT (REV)
FOXA1	GCCTGAGTTCATGTTGCTGA (FWD), AAAACGCGTATTGGAAGTGC (REV)
NR3C1	CCCAGAGCAAATGCCATAAG (FWD), GAAATGGGCAAAGGCAATAC (REV)
CTCF	CACTTCAAGCGCTATCACGA (FWD), CCTCCATTTTCCCCCTCTAC (REV)
EP300	TTAAAAATGGCCGAGAATGTG (FWD), TCTGGTAAGTCGTGCTCCAA (REV)
NFIC	CTGAACCCAGCCAGCACT (FWD), GTGTCCACGTCTTCCTCCAT (REV)
TEAD4	TCCACGAAGGTCTGCTCTTT (FWD), GTGCTTGAGCTTGTTGGATGA (REV)
TCF12	GCCTGCTGGTCACAGTGATA (FWD), GTCTTCCCGATGAGTTCCAA (REV)
CEBPB	CAGCGACGAGTACAAGATCC (FWD), AGTGCTCCACCTTCTTCTG (REV)
FOXM1	GAAGCCACTGGATGTTGGAT (FWD), AACCTGCAGCTAGGGATGTG (REV)
RAD21	GTAGAACTTTGCGGCAGCTT (FWD), TCAGCAGATGCTTCATGGTC (REV)
EGR1	CAGCACCTTCAACCCTCAG (FWD), CAGCACCTTCTCGTTGTTCA (REV)
ZBTB7A	CATGTGCACCTTCAGCTTGT (FWD), ATCTGCGAGAAGGTCATCCA (REV)
MAX	TTGAAACCTCGGTTGCTCTT (FWD), TGTGTTGTGCGGTGACTTCC (REV)
SRF	GACAGCAGCACAGACCTCAC (FWD), ATGCGGGCTAGGGTACATC (REV)
CREB1	GCGAAGGGAAATTCTTTCAA (FWD), GCACCGTTACAGTGGTGATG (REV)
TAF1	AGACTGCCCAGGAGATTGTG (FWD), CATTGGGTCCAGGCTTTCTA (REV)
USF1	ACTGTCCCCTCTTCCGTTTC (FWD), AGCACTCAGGCCTGTGAATC (REV)
YY1	AAGAAGTGGGAGCAGAAGCA (FWD), CAACCACTGTCTCATGGTCAA (REV)
REST	CAGGAGAACGCCCATATAAA (FWD), GAGGCCACATAACTGCACTG (REV)

Supplementary Table S8:

Shared ERα/FOXA1			
Top Canonical Pathways	-log ₁₀ (p-values)	Top Upstream Regulators	-log ₁₀ (p-value)
Molecular Mechanisms of Cancer	3.34	ESR1	7.06
Rac Signaling	3.28	TP63	5.52
HER-2 Signaling in Breast Cancer	3.25	TP53	4.49
Ephrin Receptor Signaling	3.22	ESR2	4.07
PPAR α / RXR α Activation	3.13	TEF	3.85
ERα only			
Top Canonical Pathways	-log ₁₀ (p-values)	Top Upstream Regulators	-log ₁₀ (p-value)
Germ Cell-Sertoli Cell Junction Signaling	4.85	beta-estradiol	7.92
Epithelial Adherens Junction Signaling	3.70	TGFB1	6.49
Ceramide Signaling	3.32	trichostatin A	6.24
Sertoli Cell-Sertoli Cell Junction Signaling	3.25	ESR1	6.11
Wnt/ β -catenin Signaling	3.02	FSH	5.92
FOXA1 only			
Top Canonical Pathways	-log ₁₀ (p-values)	Top Upstream Regulators	-log ₁₀ (p-value)
TGF- β signaling	2.94	ESR1	5.82
CD27 Signaling in Lymphocytes	2.28	beta-estradiol	5.64
Wnt/ β -catenin Signaling	2.09	dihydrotestosterone	4.48
Hereditary Breast Cancer Signaling	2.09	TP53	3.90
ATM signaling	2.09	NR3C1	3.65

